ISDN 1039-3218

Estimation of rates of sedimentation, water column mixing and porewater exchange in Port Phillip Bay using fallout and lithogenic radionuclides

G.J. Hancock, I.T. Webster and A.S. Murray
CSIRO Land and Water
Canberra, Australia

Technical Report No.47

(Consultancy Report 97-55, October 1997)

Port Phillip Bay Environmental Study
CSIRO Environmental Projects Office
Canberra, ACT, Australia

GPO Box 1666, Canberra, ACT 2601, Australia

December 1997

EXECUTIVE SUMMARY

Sedimentation

Estimates of sedimentation rates in Port Phillip Bay were made using lithogenic and fallout radionuclides. These estimates were derived from the distribution of these radionuclides in the bottom sediment profile, and from the *in situ* production and removal of ^{228}Th from the water column. Four sediment cores and a frozen slab sample were collected from four sites in the Bay in February 1996. There was good agreement in the distribution of $^{210}Pb_{ex}$ and $^{228}Th_{ex}$ in a sediment core and a frozen slab sample from the same site. This agreement, together with measurements of the $^{228}Th_{ex}$ inventory in bottom sediments, indicates that the sampling techniques had successfully recovered the top layer of sediment.

The distribution of excess ^{210}Pb ($^{210}Pb_{ex}$) in bottom sediments does not show simple exponential decrease with depth, indicating that post-depositional mixing of sediments, changes in the sedimentation rate, or both have occurred. Cs-137 has apparently been mobilised in bottom sediments, and cannot be used to determine sedimentation rates. Log-linear plots of $^{210}Pb_{ex}$ and depth indicate a rapidly mixed surface layer of 2-3 cm depth in Central Bay samples, and two regions of different slope corresponding to the 3-20 and 20-45 cm depth intervals. In the Northern Bay region, the rapidly mixed surface layer extends to about 10 cm depth.

Excess ^{228}Th ($^{228}Th_{ex}$) is present in the top 10 cm of Central Bay sediments. When the distribution of both $^{210}Pb_{ex}$ and $^{228}Th_{ex}$ are considered in combination, the sedimentation rate in the top 10 cm of sediments is constrained to be <0.9 mm/y (<0.034 g/cm^2/y). These two tracers also show that mixing of sediment is occurring to a depth of at least 10 cm in Central Bay, and probably to a depth of more than 20 cm. The mean mixing coefficient for the upper 10 cm in Central Bay is 490 ±50 mm^2/y. Below 20 cm, a different mixing regime is indicated. Evidence for bioturbation to a depth of at least 55 cm is obtained from the presence of $^{210}Pb_{ex}$ at depths of more than 70 cm. This conclusion is supported by the ^{228}Ra deficiency profile, which indicates that bioturbation and/or bioirrigation is occurring on a time scale similar to, or shorter than the ^{228}Ra half-life (5.8 y).

Measurement of ^{228}Th in the water column has enabled the determination of the residence time of particles in the water column, and hence the flux of particles to the Bay floor. At the time of sampling the mean residence time of particles in the Central Port Phillip Bay water column is 10 ±2 d. This time corresponds to a normalised particle flux of 0.15 ±0.02 g/cm^2/y in Central Bay at the time of sampling. This flux is four times the upper estimate of sedimentation derived using $^{210}Pb_{ex}$ and $^{228}Th_{ex}$, indicating that most of the suspended sediment in the water column is resuspended bottom sediment.

Water column mixing

The input of the shorter-lived Ra isotopes (^{224}Ra and ^{228}Ra) to Port Phillip Bay is dominated by their flux from bottom sediments. The water column distribution of ^{224}Ra

(half-life 3.7 d) indicates that at the time of sampling the water column was vertically well-mixed at the shallower sites (<20 m depth) on a time scale of <1.5 days. In the deeper Central Bay region there is evidence for restricted mixing of near-bottom water with overlying water. However, there is also evidence that vertical mixing of Central Bay bottom water is aided by strong (20 knot) winds.

Assuming steady state, the total flux ^{224}Ra from bottom sediments can be derived from the decay of excess ^{224}Ra in the water column. This total flux is 4 times greater than that attributable to molecular diffusion, indicating that advective exchange of porewater and surface water is a significant process in Port Phillip Bay sediments. Based on the porewater concentration of ^{224}Ra, the porewater flux in the Central Bay region is 6.8 x 10^{-5} $cm^3/cm^2/s$. If this flux is typical of the entire Bay, a volume of water approximately equal to 1.7 times the volume of Port Phillip Bay is exchanged across the sediment-water interface each year.

The standing crop of ^{228}Ra in the Port Phillip Bay water column is a balance between input from bottom sediments, and losses by decay in the water column, and by advection to Bass Strait. The flux of ^{228}Ra from bottom sediments is determined from its activity deficiency in bottom sediments with respect to its parent ^{232}Th. By determining this flux, an estimate of the residence time of water in the Bay is made. Based on the ^{228}Ra deficiency in three cores from the Central and Northern Bay regions, this time is estimated to lie in the range 234-390 days. This range could be reduced considerably by the future analysis of more sediment samples.

TABLE OF CONTENTS

Page No.

1. INTRODUCTION

Radionuclides can provide valuable information on the extent and rate of physical and biogeochemical processes occurring in estuaries and oceans. These processes include sedimentation, mixing of bottom sediments, rates of water column mixing, and the movement of water across the sediment-water interface. A major advantage of the use of radionuclides is that they act as tracers of naturally occurring processes in the environment, and so intrusive *in situ* measurement techniques are usually not required. In addition, radionuclide measurements can give a 'time averaged' signal of the process of interest, integrated over a few half-lives of the radionuclide.

This study has two main aims. The first is to determine sediment accumulation rates in Port Phillip Bay (PPB). The second is to estimate rates of water column mixing, including the exchange of water across the sediment-water interface, by measuring Ra and Th isotopes in the water column.

The presentation of results and their discussion in this report has been divided into two sections. These sections cover

- sedimentation processes, including, sediment accumulation and sediment mixing rates, water column residence time of suspended particles, and particulate fluxes to the sea floor; and

- water column mixing processes, including vertical mixing rates, surface water-porewater exchange, and the residence time of water in PPB.

The radionuclides measured in this study fall into two broad categories; fallout and lithogenic. A brief description of their origins and uses follows.

1.1. Fallout Radionuclides

The fallout radionuclides, ^{210}Pb, ^{137}Cs and ^{7}Be have been used to derive sedimentation rates occurring over time-scales ranging from months to decades (e.g. Appelby and Oldfield 1992, Sharma *et al*., 1987). These radionuclides are removed from the atmosphere by precipitation or dry deposition. Most of this fallout becomes attached to sedimentary particles. Pb-210 (half-life 22.3 y) is the most useful nuclide for determining longer-term sedimentation rates. This nuclide is formed by the decay of ^{222}Rn in the atmosphere, and can give sedimentation information pertaining to the last 60-100 y. The shortest-lived, ^{7}Be (half-life 54 d), is produced by cosmic rays, and has a useful range of about 6 months. It has been used to study short-term mixing rates of surficial bottom sediments (Krishnaswami *et al*., 1980). Cs-137 (half-life 30 y) is an artificial radionuclide, and was first detected in the atmosphere as a result of nuclear bomb testing. Providing it remains bound to sediment, the first appearance of ^{137}Cs in a sediment profile can be used as a chronological marker (Robbins and Edgington, 1975), corresponding to a date of about 1958 in the southern hemisphere (Olley *et al*., 1993).

1.2. Lithogenic Radionuclides

1.2.1. Radioactive disequilibria

Nuclides of the ^{238}U and ^{232}Th decay series (Figure 1) occur naturally in rock-forming minerals and sediments. In a closed system, the nuclides in these series eventually reach a state of secular equilibrium. In this state the activity of each member of the series is the same. The time scale for the establishment of secular equilibrium is ~10^6 y for the ^{238}U series, and ~30 y for the ^{232}Th series. However, many natural systems are not closed, and the different chemistry of the nuclides often results in radioactive disequilibria between members of a decay series (e.g. various authors in Ivanovich and Harmon, 1992). Such disequilibria is illustrated by the Th-Ra parent-daughter relationship in sediments which have been exposed to saline water (Moore 1992). Radium is much more soluble than Th in saline waters, and can be mobilised and transported away from its parent, resulting in deficiency of Ra activity at its source, and an excess at its destination. The mobility of Ra in coastal waters, together with the fact that it exists as four isotopes with a range of half-lives, has enabled it to be applied to many marine studies, such as tracing of water movement in oceans (Moore, 1992), the estimation of surface water-porewater exchange (Bollinger and Moore, 1993; Webster *et al.*, 1994; Hancock and Murray, 1996) and the estimation of water residence time in estuaries (Turekian *et al*., 1996). The particle-reactive nature of Th isotopes make them suitable for determining particle settling rates and water column residence times (Sanstchi *et al*., 1979; Nozaki *et al*., 1981), and mixing rates in surficial bottom sediments (Huh *et al*., 1987).

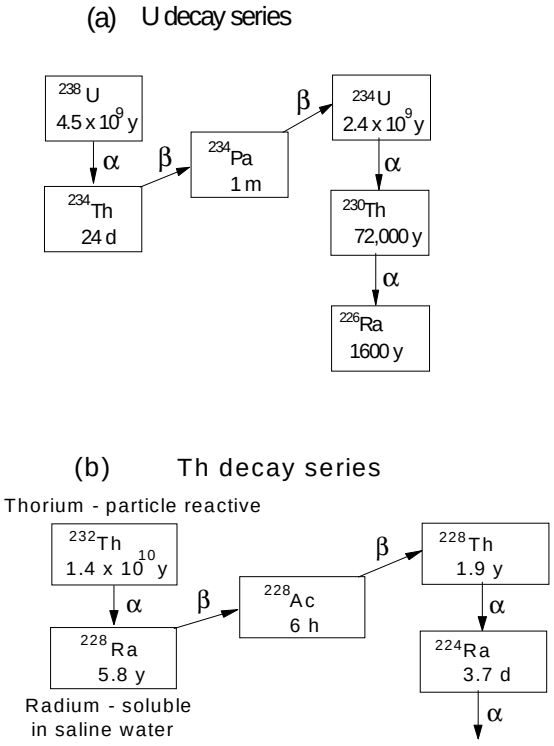

Figure 1. (a) The ^{238}U and (b) ^{232}Th decay schemes

1.2.2. Application to Port Phillip Bay

The cycling of Ra and Th in PPB is illustrated in Figure 2. Ra exists naturally in the environment as four isotopes with a range of half-lives; ^{226}Ra has a half-life ($t_{1/2}$) of 1600 y, ^{228}Ra ($t_{1/2}$ = 5.8 y), ^{223}Ra ($t_{1/2}$ = 11 d) and ^{224}Ra ($t_{1/2}$ = 3.7 d). Most of the dissolved activity of the shorter-lived Ra isotopes (^{228}Ra, ^{224}Ra and ^{223}Ra) in PPB is produced in bottom sediments by the decay of Th bound to the surface of sediment grains. Some of this Ra is then desorbed into sediment porewater, and effuses into the water column. The extent and rate of effusion gives a measure of exchange processes occurring across the sediment-water interface (section 4.2). Once in the water column, Ra acts as a conservative tracer of water movement. Since it is unsupported, the decay rate of ^{224}Ra can give an indication of the rate of water column mixing (section 4.1).

The decay of ^{228}Ra in the water column produces ^{228}Th, which is rapidly scavenged by suspended particles. The deposition of these particles onto the floor of PPB removes ^{228}Th from the water column. The production/removal equilibria which is established gives an estimate of the flux of particles to bottom sediments (section 3.3).

Most of the ^{228}Ra (and ^{226}Ra) in the water column is eventually advected to Bass Srait. By balancing this rate of advection with the flux of ^{228}Ra from bottom sediments, an estimate of the residence time of water in PPB is obtained (section 4.3).

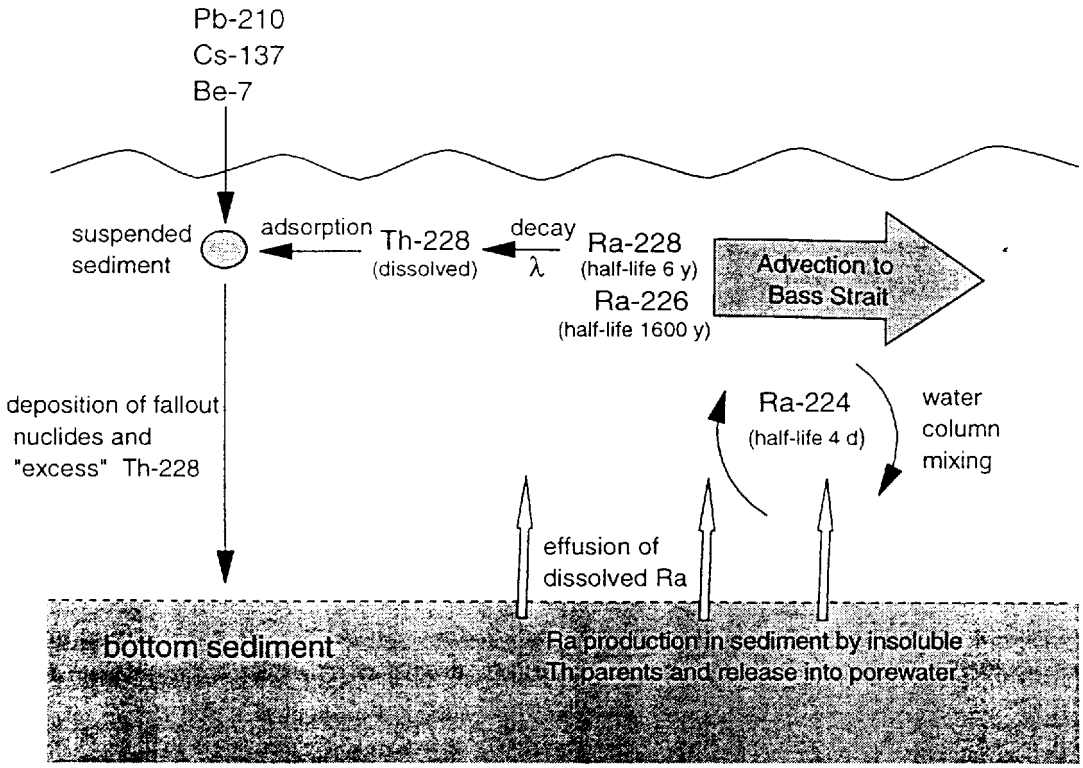

Figure 2. The fate of fallout and lithogenic (Ra and Th) nuclides in Port Phillip Bay.

2. METHODS

2.1. Sample Collection

Sampling occurred on 27 and 29 February 1996. The five sampling sites are shown in Figure 3, and their coordinates listed in Table 1. Sediment samples were collected at four sites (labelled 1-4), forming a transect from Central PPB (site 1) to Hobson's Bay in Northern PPB (site 2). Sediment core samples were collected and retrieved by divers. In addition, a vertical frozen slab of bottom sediment was collected by *in situ* freezing of sediment onto aluminium plates. The use of divers and *in situ* freezing was necessary to minimise disturbance of the sediment profile, which was highly fluid in its upper layers, and to ensure that the top of the core was recovered. The core tubes were pushed into the sediment by the divers, and the top of the tube sealed with a rubber bung. The diver then reached into the sediment and sealed the bottom of the tube with another bung. The tube was then extracted, carried to the surface in a vertical position, and packed with dry ice. The tube was kept in an upright position at all times prior to and during freezing, which occurred within one hour of collection.

Two types of core tubes were used - a perspex tube 50 cm in length and 10.5 cm in diameter, and a PVC tube 1.5 m long and 5 cm in diameter. The cores were transported intact and frozen to the Canberra laboratory for processing. The perspex cores were cut into horizontal 2 cm sections while frozen. These sections were weighed, and allowed to partially thaw. The outer 5 mm edge of the sediment section was discarded in case the coring procedure had caused smearing. The PVC cores were split in half vertically, allowed to partially thaw, and the sediment cut horizontally into 6 cm sections. Again, the outer 2-3 mm of each section was discarded.

A frozen slab sediment sample was collected at site 1. A wedge-shaped box filled with dry-ice pellets was dropped into bottom sediment from a height of about 1 m above the sea floor. Sediment then froze onto aluminium plates that had been taped to the wedge. After a pre-set time the wedge was retrieved, and the plates with the frozen sediment slab removed. The slabs of sediment were kept frozen until they reached the laboratory, where the sediment was sectioned at 2 cm depth intervals. Once again, a 2-3 mm layer of sediment contacting the plate was rejected in case of smearing.

Water samples were collected from five sites (sites 1-5, Figure 3). Surface, mid-depth and bottom water samples were taken using a Niskin bottle sampler. The bottom water samples were taken approximately 1 m above the sediment.

2.2. Laboratory Analysis

The water content of sediment was determined by drying at 50° C. The density of the sediment was determined by measuring the volume and weight of the wet sediment sample, and weighing the sediment after drying. The seawater volume is calculated from

the reduction in weight during drying, and deducted from the original wet volume to give the volume of dry sediment.

The dry sediment was measured using gamma spectrometry by the method of Murray *et al.* (1987). This technique involves the mixing of the solid sample in polyester resin, and counting using high-purity germanium detectors. It measures ^{226}Ra, ^{137}Cs, ^{7}Be, ^{228}Ra, ^{228}Th and ^{210}Pb. A subsample of the dry sediment was also measured by alpha spectromtery (Martin and Hancock, 1992). Yield tracers were added to the sample, and the sample completely dissolved by digestion with acids (HNO_3, HF, $HClO_4$). The radionuclides were then chemically isolated, and electroplated onto a metal disc. The alpha activity of the disc was counted using an ion-implanted alpha detector, and the activity of each isotope in the sample determined from the known activity of the tracer isotope. This method was used to determine Th isotopes (^{232}Th, ^{230}Th and ^{228}Th) in all samples, Ra isotopes (^{226}Ra, ^{228}Ra, ^{223}Ra and ^{224}Ra) in water samples, and ^{210}Po (as a measure of ^{210}Pb) in sediment samples. The determination of ^{210}Pb via ^{210}Po is more sensitive than the direct gamma spectrometric determination of ^{210}Pb, and ^{210}Po was used to determine excess ^{210}Pb in all sediment samples (section 3.2.3.). The activity of all nuclides was corrected for decay, and the reported activities refer to the time of collection.

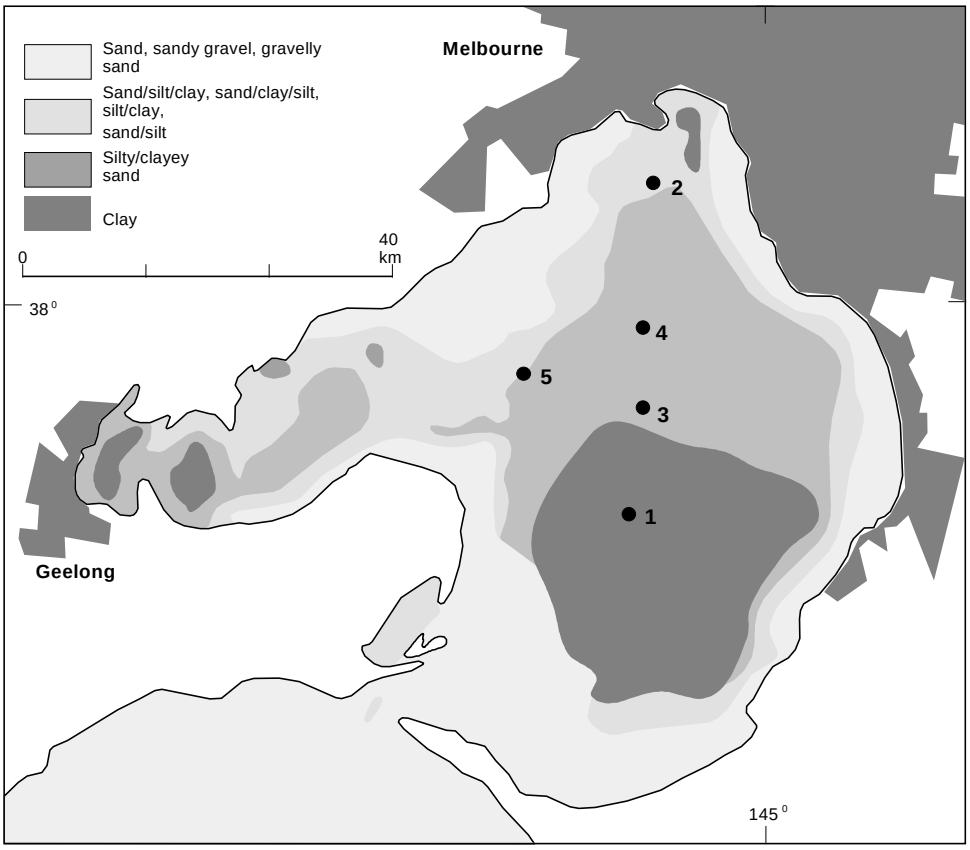

Figure 3. Sampling sites in PPB, and the distribution of sediment types (from Beasley, 1966).

Table 1. Summary of water sample data. Radionuclide activity units are mBq/L; uncertainties correspond to 1 SD.

Site (region)	Coordinates (degrees S;E)	sampling date	sample depth	Suspended sediment (mg/L)	^{226}Ra	^{228}Ra	^{224}Ra	^{232}Th	^{228}Th	$^{224}Ra_{ex}$	$^{228}Th_{a+d}$	$^{228}Th_{a+d}/^{228}Ra$ (R)	τ_{Th} (days)
1	38°09.12;	27/02/96	surface	1.9	2.5 ±0.1	19.2 ±2.4	4.5 ±1.4	0.08 ±0.03	0.34 ±0.07	4.1 ±1.4	0.26 ±0.08	0.014 ±0.004	13.8 ±4.4
(Central)	144°54.40		12	1.4	2.5 ±0.2	19.0 ±1.4	3.0 ±0.9	0.02 ±0.01	0.20 ±0.04	2.8 ±0.9	0.18 ±0.04	0.009 ±0.002	9.6 ±2.3
			24	3.8	2.5 ±0.2	19.8 ±1.6	10.7 ±1.2	0.15 ±0.02	0.37 ±0.05	10.3 ±1.2	0.22 ±0.05	0.011 ±0.003	11.3 ±2.9
2	37°54.12;	27/02/96	surface	3.3	2.4 ±0.1	16.0 ±0.8	6.1 ±0.7	0.09 ±0.02	0.34 ±0.04	5.8 ±0.7	0.25 ±0.04	0.016 ±0.003	16.0 ±2.8
(Northern)	144°54.30		6.5	2.5	2.3 ±0.1	17.7 ±1.1	4.7 ±0.6	0.04 ±0.02	0.22 ±0.04	4.5 ±0.7	0.18 ±0.04	0.010 ±0.003	10.3 ±2.6
			12	7.9	2.7 ±0.3	18.9 ±2.2	6.5 ±1.5	0.22 ±0.05	0.98 ±0.11	5.5 ±1.5	0.76 ±0.12	0.040 ±0.008	42.2 ±8.3
3	38°06.05;	29/02/96	surface	1.5	2.3 ±0.2	14.6 ±1.3	2.1 ±0.4	0.01 ±0.02	0.12 ±0.02	1.9 ±0.5	0.11 ±0.03	0.008 ±0.002	7.6 ±1.9
(Central)	144°54.19		12	1.9	2.7 ±0.2	18.6 ±1.1	4.0 ±0.6	0.05 ±0.02	0.29 ±0.03	3.7 ±0.6	0.24 ±0.03	0.013 ±0.002	13.2 ±2.0
			23	1.8	2.7 ±0.2	17.1 ±1.5	4.4 ±0.8	0.03 ±0.01	0.17 ±0.03	4.2 ±0.7	0.14 ±0.03	0.008 ±0.002	8.1 ±2.0
4	38°01.21;	29/02/96	surface	2.8	2.3 ±0.2	15.4 ±1.8	3.5 ±0.6	0.11 ±0.02	0.35 ±0.04	3.2 ±0.6	0.24 ±0.04	0.016 ±0.003	15.9 ±3.5
(Northern/	144°54.19		9	1.9	2.1 ±0.1	15.3 ±0.7	3.2 ±0.5	0.04 ±0.01	0.28 ±0.05	3.0 ±0.5	0.24 ±0.03	0.016 ±0.002	16.0 ±2.3
Central)			18	1.9	3.3 ±0.2	18.4 ±1.4	4.2 ±0.6	0.03 ±0.02	0.22 ±0.05	4.0 ±0.6	0.19 ±0.06	0.010 ±0.003	10.5 ±3.1
5	38°03.35;	29/02/96	surface	2.5	2.4 ±0.2	15.7 ±1.1	3.2 ±0.4	0.08 ±0.02	0.23 ±0.04	3.0 ±0.4	0.15 ±0.04	0.010 ±0.003	9.7 ±2.7
(Surround/	144°45.77		7.5	2.9	2.5 ±0.1	14.7 ±1.0	2.8 ±0.4	0.06 ±0.02	0.23 ±0.04	2.6 ±0.4	0.17 ±0.04	0.011 ±0.003	11.4 ±3.2
Central)			14	2.9	2.7 ±0.2	16.2 ±1.2	3.1 ±0.5	0.03 ±0.02	0.17 ±0.05	2.9 ±0.5	0.14 ±0.05	0.009 ±0.003	8.8 ±3.4

3. SEDIMENTATION STUDY

The Central Bay area of PPB has the greatest water column depth (~25 m) and the thickest layer of deposited sediments (~2 m; Harris *et al.*, 1996), and it was expected that cores from this area would provide the least disturbed long-term record of sedimentation in the bay. Four sediment samples were selected for detailed analysis from two sites in Central Bay. Two samples were analysed from site 1; a short core (SC1, depth 43 cm) and the frozen slab sample (FS1, depth 35 cm). These samples were selected to compare the sediment profiles obtained by two different sampling techniques, in case either technique had resulted in mixing or loss of surface sediment. Two cores were collected from site 3, a short core (SC3, depth 44 cm) and a longer core (LC3, depth 127 cm).

One core was selected for analysis from Northern PPB (site 2, Hobson's Bay). The water depth in this area is ~13 m, and sediment thickness is estimated to be about 0.5 m. The core selected for analysis (SC2) was about 36 cm long.

Data for the five sediment profiles are summarised in Tables 2-6. Radionuclide data are expressed as mBq/g dry weight of sediment.

3.1. Physical Characteristics of Bottom Sediment

The sediment in all cores from Central PPB was predominantly fine silt and clay. The cores appeared homogeneous, with no visible stratification. The porosity (ϕ) of the cores is related to water content by

$$\phi = \frac{w}{\left[w + \left((100 - w)/\rho_d\right)\right]}$$

where w is the percentage weight of water in the wet sediment, and ρ_d is the dry sediment density. The value of ρ_d in Central PPB cores did not vary significantly with depth, or between cores. Its mean value was 1.88 g/cm^3. The relationship between ϕ and depth in LC3 is shown in Figure 4. The value of ϕ is highest at the surface (~0.84), and decreased with depth (0.72 at 1.2 m), indicating increased compaction of the sediment. This trend is typical of other cores from Central PPB.

The physical characteristics of the Northern Bay core (SC2) differed from Central PPB, having higher ρ_d (2.28-2.54), and higher sand content. The change in ϕ with depth is also more marked in this core (Figure 4), ranging from 0.77 at the surface, to 0.34 at 36 cm depth.

Table 2. Core SC1 summary (The uncertainties in the radionuclide activities are derived from counting statistics only).

depth	water content	porosity	Th-230	Ra-226	Pb-210	Pb-210ex	Cs-137	Be-7	Th-232	Ra-228	Th-228	Th-228ex	Ra-228 AR Th-232
(cm)	(%)		(mBq/g dry weight)										
1.4	72.7	0.83	33.8 ± 1.4	15.9 ± 1.0	50.5 ± 1.7	34.6 ± 2.0	2.3 ± 0.7	12.4 ± 4.5	50.5 ± 1.8	38.7 ± 2.3	56.3 ± 1.3	17.6 ± 2.6	0.77 ± 0.05
3.7	72.2	0.83	37.8 ± 2.1	17.4 ± 0.8	55.5 ± 1.4	38.1 ± 1.6	1.6 ± 0.5	0.8 ± 3.9	54.5 ± 2.9	35.3 ± 1.7	46.7 ± 0.9	11.4 ± 1.9	0.65 ± 0.05
5.6	68.6	0.80	36.6 ± 1.7	17.0 ± 1.1	49.0 ± 1.8	32.0 ± 2.1	1.3 ± 0.7	-1.8 ± 4.9	55.6 ± 2.3	39.8 ± 2.5	42.7 ± 1.3	2.9 ± 2.8	0.72 ± 0.05
7.7	70.3	0.82	35.4 ± 1.7	17.1 ± 1.0	44.0 ± 1.5	26.9 ± 1.8	2.5 ± 0.7		52.9 ± 2.2	36.2 ± 2.4	40.6 ± 1.2	4.4 ± 2.7	0.68 ± 0.05
9.7	68.0	0.80	35.3 ± 1.3	18.9 ± 1.0	37.8 ± 1.5	18.9 ± 1.8	1.6 ± 0.7		54.1 ± 1.7	47.1 ± 2.4	42.8 ± 1.2	-4.3 ± 2.7	0.87 ± 0.05
11.7	69.4	0.81	35.5 ± 1.6	20.3 ± 0.7	38.6 ± 1.5	18.3 ± 1.7	3.1 ± 0.6		56.8 ± 2.2	44.9 ± 1.7	44.2 ± 0.9	-0.7 ± 1.9	0.79 ± 0.04
13.8	69.4	0.81	36.2 ± 1.6	18.1 ± 1.0	34.5 ± 1.0	16.4 ± 1.4	2.9 ± 0.7		54.6 ± 2.1	42.2 ± 2.3	42.3 ± 1.1	0.1 ± 2.5	0.77 ± 0.05
15.8	67.8	0.80	36.9 ± 1.8	18.1 ± 0.6	33.4 ± 1.0	15.3 ± 1.2	2.1 ± 0.4		54.0 ± 2.4	41.9 ± 1.3	43.1 ± 0.8	1.2 ± 1.5	0.78 ± 0.04
17.8	65.8	0.78		20.1 ± 0.8			2.1 ± 0.5			47.7 ± 1.8	44.6 ± 1.0	-3.1 ± 2.1	
19.8	67.0	0.79	39.8 ± 2.1	20.9 ± 0.9	30.2 ± 0.8	9.3 ± 1.2	2.0 ± 0.6		62.9 ± 3.0	50.5 ± 2.1	47.6 ± 1.1	-2.9 ± 2.4	0.80 ± 0.05
23.9	68.3	0.80		18.2 ± 0.9	29.1 ± 1.0	10.9 ± 1.3	1.5 ± 0.7			47.0 ± 2.3	45.6 ± 1.2	-1.4 ± 2.6	
28.0	67.6	0.80	36.5 ± 1.4	18.9 ± 0.5	26.6 ± 0.9	7.7 ± 1.0	2.7 ± 0.5		56.3 ± 1.9	49.8 ± 1.4	48.4 ± 0.8	-1.4 ± 1.6	0.88 ± 0.04
32.1	64.5	0.77		15.6 ± 5.4	32.3 ± 1.1		2.4 ± 0.6			46.6 ± 1.7	43.3 ± 0.8	-3.3 ± 1.9	
36.0	65.5	0.78	38.5 ± 1.5	19.7 ± 0.9	26.2 ± 0.8	6.5 ± 1.2	1.8 ± 0.8		59.8 ± 2.0	48.7 ± 2.4	50.0 ± 1.1	1.3 ± 2.6	0.81 ± 0.05
40.3	64.2	0.77		17.0 ± 0.8	21.0 ± 0.9	4.0 ± 1.2	1.2 ± 0.7			47.9 ± 2.2	46.9 ± 1.1	-1.0 ± 2.5	
44.8	66.3	0.79	36.7 ± 1.7	17.8 ± 0.5	23.9 ± 0.6	6.1 ± 0.8	1.5 ± 0.3		55.5 ± 2.4	50.6 ± 1.2	48.4 ± 0.7	-2.2 ± 1.4	0.91 ± 0.04

Table 3. Frozen slab samples FS1 summary.

depth (cm)	water content (%)	porosity	Ra-226	Pb-210	Pb-210ex	Cs-137	Ra-228	Th-228	Th-228ex
			(mBq/g dry weight.)						
1	78.5	0.87	18.6 ± 2.7	52.6 ± 2.2	34.0 ± 3.5	0.5 ± 1.9	47.8 ± 7.0	67.1 ± 2.8	28.6 ± 11.2
3	75.2	0.85	22.0 ± 1.9	60.4 ± 1.9	38.4 ± 2.7	2.5 ± 1.2	41.4 ± 4.8	64.2 ± 2.2	25.7 ± 6.0
5	72.3	0.83	17.0 ± 1.0	53.6 ± 1.6	36.6 ± 1.9	2.9 ± 0.7	38.0 ± 2.4	47.3 ± 1.2	13.8 ± 3.6
7	70.1	0.82	17.4 ± 0.9	50.5 ± 1.4	33.1 ± 1.7	2.5 ± 0.6	39.4 ± 2.1	45.1 ± 1.2	7.5 ± 3.2
9	70.0	0.81	18.8 ± 1.0	45.9 ± 1.4	27.1 ± 1.7	1.6 ± 0.6	37.3 ± 2.5	43.2 ± 1.3	8.7 ± 4.1
11	70.8	0.82	17.3 ± 0.7	41.5 ± 1.4	24.2 ± 1.6	1.8 ± 0.5	38.1 ± 1.7	36.8 ± 1.0	-1.3 ± 2.0
13	70.2	0.82	15.4 ± 0.9	35.2 ± 5.7	19.8 ± 5.8	2.0 ± 0.6	40.2 ± 2.3	37.1 ± 1.1	-3.1 ± 2.5
15	68.9	0.81	17.7 ± 1.3	36.3 ± 1.3	18.6 ± 1.8	1.2 ± 0.9	36.2 ± 3.4	40.2 ± 1.5	4.0 ± 3.7
17	68.5	0.80	16.2 ± 1.4	31.3 ± 8.5	15.1 ± 8.6	2.9 ± 0.9	39.2 ± 3.6	40.1 ± 1.5	0.9 ± 3.9
19	66.0	0.78	19.9 ± 1.6	33.5 ± 1.2	13.6 ± 2.0	2.6 ± 1.1	42.6 ± 4.1	41.4 ± 1.7	-1.2 ± 4.4
21	67.8	0.80							
23	68.6	0.80	15.9 ± 2.0	31.4 ± 1.0	15.5 ± 2.2	1.9 ± 1.4	30.3 ± 5.2	42.0 ± 2.0	11.7 ± 5.6
25	68.4	0.80							
27	67.3	0.79	18.9 ± 1.4	27.4 ± 1.0	8.5 ± 1.7	1.2 ± 0.9	40.6 ± 3.5	43.8 ± 1.5	1.7 ± 3.2
29	67.7	0.80							
31	67.7	0.80	18.0 ± 1.8	27.4 ± 1.0	9.4 ± 2.1	3.3 ± 1.2	41.2 ± 4.6	45.7 ± 1.9	4.5 ± 5.0
33	66.7	0.79							
35	65.5	0.78	16.9 ± 1.6	25.0 ± 0.8	8.1 ± 1.8	1.9 ± 1.1	51.8 ± 4.3	57.8 ± 2.0	6.0 ± 4.7

Table 4. Core SC3 summary.

depth (cm)	water content (%)	porosity	Th-230	Ra-226	Pb-210	Pb-210ex	Cs-137	Be-7	Th-232	Ra-228	Th-228	Th-228ex	Ra-228 AR Th-232
			(mBq/g dry weight.)										
0.15	76.3	0.86		14.8 ± 0.7	47.0 ± 1.6	32.2 ± 1.7							
0.85	76.3	0.86	37.1 ± 1.6	17.6 ± 0.8	52.1 ± 1.6	34.5 ± 1.8	1.3 ± 0.6	5.0 ± 3.8	54.2 ± 2.0	36.0 ± 2.0	54.1 ± 1.2	18.1 ± 2.3	0.66 ± 0.04
3.2	72.2	0.83		16.9 ± 0.7	46.9 ± 1.3	30.0 ± 1.5	2.2 ± 0.6	2.8 ± 3.6		34.2 ± 1.8	46.0 ± 1.0	11.8 ± 2.0	
5.3	69.2	0.81	36.3 ± 1.7	19.7 ± 1.1	45.3 ± 1.3	25.6 ± 1.7	2.9 ± 0.9	0.0 ± 4.4	56.8 ± 2.3	43.9 ± 2.6	51.1 ± 1.3	7.2 ± 2.9	0.77 ± 0.06
7.4	67.9	0.8	37.2 ± 1.7	18.0 ± 0.8	42.0 ± 1.6	24.0 ± 1.8	2.7 ± 0.7		58.9 ± 2.4	37.5 ± 2.0	43.5 ± 1.0	6.0 ± 2.2	0.64 ± 0.04
9.4	67.2	0.79		19.0 ± 1.0			3.3 ± 0.8			45.0 ± 2.4	45.8 ± 1.2	0.9 ± 2.7	
11.5	67	0.79	37.3 ± 2.2	18.9 ± 0.6	35.6 ± 1.0	16.7 ± 1.2	3.3 ± 0.5		57.4 ± 2.2	44.9 ± 1.5	46.3 ± 0.9	1.5 ± 1.7	0.78 ± 0.04
13.5	67.5	0.8		19.3 ± 0.6			1.9 ± 0.4			43.3 ± 1.4	42.4 ± 0.8	-0.9 ± 0.8	
15.6	67.6	0.8	42.2 ± 1.9	18.5 ± 0.6	34.5 ± 1.1	16.0 ± 1.3	1.6 ± 0.5		60.8 ± 2.5	42.6 ± 1.4	41.8 ± 0.7	-0.8 ± 0.7	0.7 ± 0.04
19.7	66.3	0.79	41.1 ± 1.7	18.2 ± 1.0	33.2 ± 1.1	15.0 ± 1.5	2.4 ± 0.7		59.5 ± 2.2	48.3 ± 2.4	44.4 ± 1.2	-3.9 ± 1.2	0.81 ± 0.05
23.8	66.6	0.79	39.9 ± 2.1	19.6 ± 0.9	30.2 ± 1.1	10.6 ± 1.4	2.4 ± 0.6		57.1 ± 2.6	46.0 ± 2.1	45.6 ± 1.1	-0.4 ± 1.1	0.81 ± 0.05
27.9	66.7	0.79	35.3 ± 2.1	15.7 ± 0.6	29.4 ± 0.6	13.7 ± 0.8	2.3 ± 0.5		58.4 ± 2.6	40.1 ± 1.5	39.6 ± 0.7	-0.5 ± 0.7	0.69 ± 0.04
31.9	65.4	0.78		20.9 ± 0.9			2.1 ± 0.7			48.8 ± 2.1	46.1 ± 1.1	-2.7 ± 1.1	
33.9	65	0.78	39.2 ± 2.5	18.7 ± 0.5	27.0 ± 0.7	8.3 ± 0.9	2.3 ± 0.4		58.7 ± 2.5	44.8 ± 1.2	45.1 ± 0.7	0.3 ± 0.7	0.76 ± 0.04
37.9	65.1	0.78		19.0 ± 0.6			3.2 ± 0.5			49.7 ± 1.5	47.8 ± 0.9	-1.9 ± 0.9	
43.3	62.7	0.76	36.2 ± 1.9	16.4 ± 0.5	26.8 ± 0.8	10.4 ± 0.9	2.0 ± 0.4		52.0 ± 2.4	43.2 ± 1.2	41.6 ± 0.7	-1.6 ± 0.7	0.83 ± 0.04

Table 5. Core LC3 summary.

depth (cm)	water content (%)	porosity	Th-230	Ra-226	Pb-210	Pb-210ex	Cs-137	Ra-228	Th-228	Ra-228 AR Th-232
			(mBq/g dry weight.)							
3	74.3	0.84	33.8 ± 1.8	20.5 ± 2.4	45.0 ± 1.4	24.5 ± 2.8	4.0 ± 1.6	54.7 ± 2.5	41.7 ± 2.5	51.0 ± 2.4
9	69.2	0.81	35.8 ± 1.9	20.1 ± 1.9	45.4 ± 1.1	25.3 ± 2.2	2.2 ± 1.2	56.2 ± 1.8	46.5 ± 4.7	55.7 ± 2.0
15	68.5	0.80	39.9 ± 2.2	19.7 ± 1.6	45.5 ± 1.1	25.8 ± 1.9	4.6 ± 1.3	55.9 ± 2.8	42.8 ± 3.8	46.0 ± 2.5
21	67.4	0.80	36.3 ± 2.6	18.2 ± 1.1	38.1 ± 1.0	19.9 ± 1.5	2.4 ± 0.9	58.2 ± 2.6	48.4 ± 2.6	50.7 ± 2.4
27	65.6	0.78	36.2 ± 3.2	19.4 ± 0.6	28.3 ± 1.1	8.9 ± 1.3	2.5 ± 0.5	53.8 ± 4.1	50.4 ± 1.5	49.4 ± 3.9
33	64.7	0.78	36.3 ± 2.2	19.4 ± 0.5	27.7 ± 1.0	8.3 ± 1.1	2.3 ± 0.3	55.1 ± 2.9	47.9 ± 1.3	44.4 ± 2.5
39	63.6	0.77	33.2 ± 2.2	19.7 ± 0.5	27.3 ± 0.8	7.6 ± 0.9	1.3 ± 0.5	56.6 ± 3.2	48.6 ± 1.4	46.5 ± 2.9
45	62.0	0.75	35.6 ± 2.1	18.4 ± 0.5	27.3 ± 1.0	8.9 ± 1.1	2.4 ± 0.4	58.8 ± 2.9	49.8 ± 1.3	49.2 ± 2.6
57	64.0	0.77	35.8 ± 1.9	19.9 ± 0.5	23.3 ± 0.8	3.4 ± 0.9	1.8 ± 0.4	60.1 ± 2.7	50.9 ± 1.2	49.4 ± 2.3
69	62.7	0.76	35.1 ± 2.4	19.0 ± 0.5	21.8 ± 0.6	2.8 ± 0.8	1.4 ± 0.4	55.9 ± 3.2	54.7 ± 1.2	52.9 ± 3.2
81	63.0	0.76	38.7 ± 2.2	18.4 ± 0.5	18.6 ± 0.6	0.2 ± 0.8	1.2 ± 0.3	61.5 ± 3.0	54.7 ± 1.3	54.7 ± 2.8
87	60.7	0.74	37.1 ± 1.5	20.4 ± 1.1			-0.3 ± 0.8	55.8 ± 2.0	49.1 ± 2.7	49.1 ± 1.8
93	60.6	0.74	45.7 ± 1.8	19.2 ± 0.4	19.1 ± 2.4	-0.1 ± 2.4	0.5 ± 0.3	60.4 ± 2.3	55.2 ± 1.1	55.2 ± 2.3
105	60.8	0.74	38.1 ± 2.4	19.2 ± 0.5	17.6 ± 0.7	-1.6 ± 0.9	0.1 ± 0.4	54.0 ± 3.0	54.1 ± 1.3	57.0 ± 3.1
117	59.9	0.74	36.5 ± 2.4	22.5 ± 0.7	20.4 ± 0.6	-2.1 ± 0.9	0.1 ± 0.4	55.5 ± 3.1	60.1 ± 1.8	52.6 ± 3.1
124	57.7	0.72	38.8 ± 2.6	22.5 ± 0.4	20.7 ± 0.7	-1.8 ± 0.8	0.4 ± 0.3	59.6 ± 3.5	55.0 ± 1.1	53.9 ± 3.3

Table 6. Core SC2 summary

depth (cm)	water content (%)	porosity	Th-230	Ra-226	Pb-210	Pb-210 ex	Cs-137	Th-232	Ra-228	Th-228	Ra-228 AR Th-232
			(mBq/g dry weight.)								
0.5	57.1	0.71	23.1 ± 0.9	22.0 ± 0.9	38.7 ± 1.0	16.7 ± 1.3	1.5 ± 0.6	39.3 ± 1.3	34.4 ± 2.0	41.2 ± 1.0	0.88 ± 0.06
1.7	50.8	0.66	22.2 ± 1.0	18.0 ± 0.9	39.0 ± 1.6	21.0 ± 1.8	1.2 ± 0.7	38.5 ± 1.3	30.4 ± 2.2	34.6 ± 1.0	0.79 ± 0.06
2.9	46.8	0.62		17.2 ± 0.8			0.8 ± 0.4		31.4 ± 1.7	33.3 ± 0.8	
4.2	43.9	0.60	22.1 ± 0.7	19.8 ± 0.8	33.2 ± 1.1	13.4 ± 1.4	2.6 ± 0.6	39.7 ± 1.1	35.0 ± 1.9	36.3 ± 1.0	0.88 ± 0.05
5.4	41.4	0.57		18.2 ± 0.7			1.3 ± 0.4		30.2 ± 1.5	34.0 ± 0.8	
6.7	40.7	0.56	20.7 ± 0.9	17.5 ± 0.9	31.1 ± 1.5	13.6 ± 1.7	0.7 ± 0.7	36.8 ± 1.3	29.2 ± 2.0	31.6 ± 0.9	0.79 ± 0.06
7.9	38.9	0.54		17.9 ± 0.8			1.3 ± 0.6		35.6 ± 1.9	33.3 ± 0.9	
9.2	37.5	0.53	18.9 ± 0.8	18.2 ± 0.4	31.9 ± 1.2	13.7 ± 1.3	1.6 ± 0.3	36.7 ± 1.2	31.8 ± 0.9	35.1 ± 0.5	0.87 ± 0.04
11	37.2	0.53		16.8 ± 0.6			1.1 ± 0.4		33.4 ± 1.4	34.1 ± 0.8	
13	38	0.54	21.5 ± 1.0	18.7 ± 0.4	29.3 ± 1.2	10.6 ± 1.3	1.5 ± 0.2	37.3 ± 0.1	35.3 ± 0.9	35.4 ± 0.5	0.95 ± 0.02
15	34.3	0.50		17.1 ± 0.3			1.6 ± 0.2		32.6 ± 0.7	33.1 ± 0.4	
18	33.2	0.48	21.1 ± 0.8	16.7 ± 0.3	24.5 ± 1.0	7.8 ± 1.0	1.2 ± 0.2	38.1 ± 1.1	33.0 ± 0.7	33.3 ± 0.4	0.87 ± 0.03
20	32.7	0.48		17.2 ± 0.5			1.0 ± 0.3		30.8 ± 1.1	32.7 ± 0.7	
22	29.7	0.44	17.9 ± 0.8	16.4 ± 0.2	20.0 ± 1.0	4.5 ± 1.0	1.1 ± 0.1	31.6 ± 1.1	30.6 ± 0.5	32.0 ± 0.4	0.97 ± 0.04
24	29.8	0.44		16.1 ± 0.2			1.0 ± 0.1		32.6 ± 0.5	32.2 ± 0.4	
27	28.3	0.43	26.9 ± 1.1	16.3 ± 0.3	20.8 ± 0.9	3.4 ± 0.9	0.9 ± 0.2	32.8 ± 1.2	30.5 ± 0.8	31.9 ± 0.6	0.93 ± 0.04
31	25.6	0.39		14.8 ± 0.2			0.7 ± 0.2		27.6 ± 0.6	29.5 ± 0.4	
35	23.6	0.37	17.7 ± 0.8	16.1 ± 0.3	16.8 ± 0.7	0.7 ± 0.8	1.0 ± 0.1	27.6 ± 1.0	31.6 ± 0.6	31.7 ± 0.4	1.14 ± 0.05

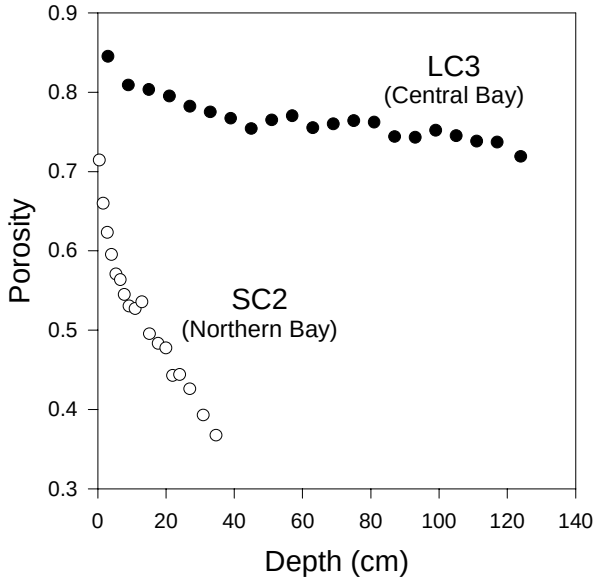

Figure 4. Porosity as a function of depth in cores from Central and Northern PPB

3.2. Radionuclide Distribution in Sediments

3.2.1. Be-7

Be-7 was only detected in the top 2.7 cm of core SC1 (12 ±5 mBq/g). Given its short half-life (53 d), ^{7}Be was not expected to yield sedimentation information. However it can be used to give an indication of the rapidity of sediment mixing. When the ^{7}Be measurement uncertainties are considered (±4 mBq/g), it is clear that if sediment mixing is occurring in the top 2 sections (the top 4.6 cm) of core SC1, it is occurring on a time scale equal to or longer than one half-life of ^{7}Be.

3.2.2. Cs-137

Cs-137 is detected throughout the short cores SC1 and SC3 (depth ~43 cm), and to a depth of about 80 cm in LC3. If ^{137}Cs has remained physically and chemically immobile in the sediment, its detection would correspond to a date no earlier than 1958. This gives a maximum age of about 40 years for sediment at a depth of 80 cm, corresponding to an average sedimentation rate of 20 mm/y over the last 40 years. However, the diffusion of solutes in sediments is affected by the strength of their adsorption to sediment grains (Lerman and Lietzke, 1975; also section 4.2.2), and Cs adsorption may be relatively weak in highly porous, saline sediments, such as those in Central PPB. In LC3, ^{137}Cs is present below the depth at which $^{210}Pb_{ex}$ is measurable (Figure 5), corresponding to an age of at least four ^{210}Pb half-lives (~90 years). This observation can only be explained by the desorption of ^{137}Cs into porewater and its diffusion into deeper sediment, rendering it of little use for sedimentation studies.

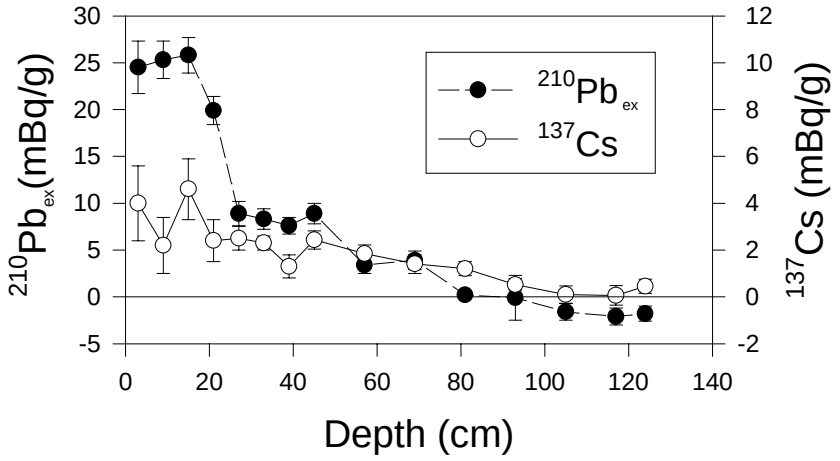

Figure 5. $^{210}Pb_{ex}$ and ^{137}Cs in LC3. ^{137}Cs activity (right vertical axis) is detected at a greater depth than $^{210}Pb_{ex}$, indicating that it has been mobilised.

3.2.3. Pb-210

There is no significant difference between the ^{210}Pb profile in the frozen slab sample (FS1) and the short core (SC1) taken at site 1, indicating that both collection techniques had recovered the surficial sediment, and that there had been little or no disturbance of the core profile during sampling. Further evidence for the complete recovery of surficial sediments is provided by the $^{228}Th_{ex}$ inventory (section 3.3.2).

The ^{226}Ra activity is relatively constant with depth in all sediment samples, generally lying in the range 15-20 mBq/g. It is generally assumed that net losses of the gaseous daughter of ^{226}Ra (^{222}Rn) from bottom sediments are small. If this assumption is valid, the ^{226}Ra activity of the sediment gives the activity of supported ^{210}Pb activity. The level of unsupported ^{210}Pb, or 'excess' ^{210}Pb activity ($^{210}Pb_{ex}$) is given by the difference between the ^{226}Ra and ^{210}Pb activities. With increasing depth the ^{210}Pb activity should decrease as a result of radioactive decay, approaching the ^{226}Ra activity at infinite depth. Hence $^{210}Pb_{ex}$ activity should approach zero with increasing depth.

In the ideal situation, where ^{210}Pb in bottom sediments remains physically and chemically immobile, and where sedimentation rate and sediment wet density remains constant with depth, a plot of $^{210}Pb_{ex}$ against depth should approximate the form $y = Ae^{-bx}$. A least squares linear regression of a log-linear plot of $^{210}Pb_{ex}$ against depth would then yield a slope of -2.303*b*. The sedimentation rate, *r* (mm/y) is determined from λ/b, where λ is the decay constant of ^{210}Pb, given by $\ln 2/t_{1/2}$ (Appleby and Oldfield, 1992). If the sediment wet density changes with depth due to compaction or changes in the sediment characteristics, a log-linear plot of $^{210}Pb_{ex}$ against cumulative dry mass, rather than depth, should be used to determine *r*. In this case *r* has units of $g/cm^2/y$. For all Central Bay samples, the change in sediment wet density with depth (as derived from by ϕ and ρ_d) is small in the 0-45 cm depth interval, and $^{210}Pb_{ex}$ has been plotted against depth (Figure 6). The Northern Bay core (SC2) shows significant

changes in sediment wet density with depth, and $^{210}Pb_{ex}$ has been plotted against cumulative dry mass (Figure 7).

The $^{210}Pb_{ex}$ activity in SC1 (Figure 6) decreases from about 36 mBg/g in the top 3 cm of the core, to 6.1 ±0.8 mBq/g at the base of the core (45 cm depth). This decrease can be represented by three areas of different slope, corresponding to the upper 3 cm, 3-20 cm, and 20-45 cm depth regions. Regions of variable slope occur at all sites, suggesting that a change in sedimentation rate may have occurred. If this is the case, the proper interpretation of these plots requires the selection of a suitable dating model. The rationale for model selection is outlined in the following section (3.2.4). However, the non-linear segments may also be due to different regimes of post-depositional mixing of bottom sediment. For example, mixing which occurs on a time scale which is rapid compared with the half-life of ^{210}Pb would result in relatively constant concentrations of $^{210}Pb_{ex}$, such as occurs in the top 2 or 3 cm of the Central Bay sediments, and the top 10 cm of SC2. Slower mixing can result in exponential decrease of $^{210}Pb_{ex}$ with depth, as is seen in the 3-20 and 20-45 cm depth intervals. Neglect of this mixing will lead to an over-estimation of sedimentation rates if these rates are based solely on radioactive decay of ^{210}Pb (Robbins, 1978). The extent and rate of mixing in PPB cores is discussed below in section 3.3.

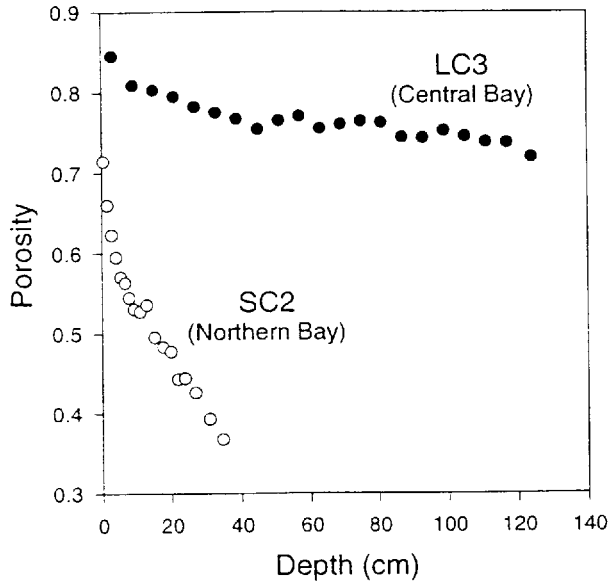

Figure 6. Central Bay depth profiles from site 1 (top) and site 3. The apparent sedimentation rates are shown for each linear regression segment for the short cores. As discussed in the text, these rates are upper estimates due to the effects of sediment mixing. Linear regression has not been applied to LC3.

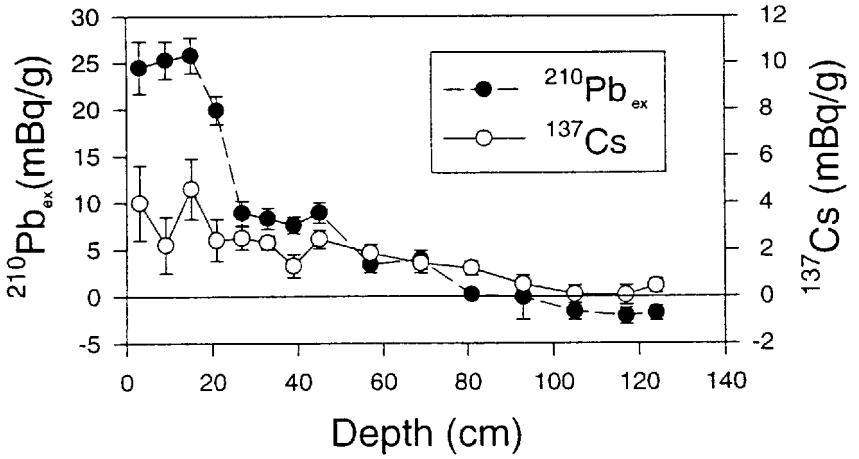

Figure 7. Northern Bay core (site 2). Due to changing wet sediment density with depth, $^{210}Pb_{ex}$ in this core is plotted against cumulative dry mass.

Selection of dating models

Two models are commonly used to date sediments with apparent variable sedimentation rates. These are termed the constant initial concentration (CIC) model, and the constant rate of supply (CRS) model (Appelby and Oldfield, 1992). The CIC model assumes that the concentration of ^{210}Pb in depositing sediment has remained constant, with consequent variation of ^{210}Pb flux with changes in sedimentation rate. The CRS model assumes constant flux, which means that the ^{210}Pb concentration will vary as sedimentation rate changes.

When selecting the appropriate dating model, the sources of $^{210}Pb_{ex}$ must be considered. Major sources are likely to be fallout ^{210}Pb from the atmosphere, and $^{210}Pb_{ex}$ associated with fluvial sediments. A third source, *in situ* production of ^{210}Pb in the PPB water column by dissolved ^{226}Ra is small compared with atmospheric fallout, and can be ignored. The parameter that helps to determine the relative contribution of the two main sources is the inventory (I_{Pb}) of $^{210}Pb_{ex}$ in bottom sediments. A close agreement between I_{Pb} and the calculated standing crop of $^{210}Pb_{ex}$ due to atmospheric flux would normally indicate that direct atmospheric deposition is the main source of $^{210}Pb_{ex}$ to the sediments, and the CRS model is likely to be the best choice. However, if I_{Pb} is much higher than predicted by atmospheric deposition, a significant fraction of $^{210}Pb_{ex}$ may have been delivered in association with sediment transported from the catchment. In this case the flux of $^{210}Pb_{ex}$ could vary, and the CIC model may be appropriate. The sediment inventory (I) of a species is determined from

$$I = \sum_{i=1}^{\infty} c_i m_i \qquad (1)$$

where, in this case, c_i is the $^{210}Pb_{ex}$ concentration of sediment in depth section i, and m_i is the mass of sediment per unit area (g/cm^2) in that section. From the distribution of $^{210}Pb_{ex}$ in core LC3, the value of I_{Pb} at site 3 is 330 mBq/cm^2. Only LC3 data can be used to determine I_{Pb} in Central Bay, since unsupported ^{210}Pb exists at the base of the shorter cores. The $^{210}Pb_{ex}$ inventory in Northern PPB can be determined from SC2. This value (350 mBq/cm^2) is similar to Central PPB.

The estimated standing crop of $^{210}Pb_{ex}$ due to atmospheric fallout in the PPB region is 160-200 mBq/cm^2 (Turekian *et al.*, 1977), which is only 50-60% of I_{Pb} in Central Bay. The the remaining 40-50% must therefore have another source. Some of this extra $^{210}Pb_{ex}$ must have come directly from the catchment, and/or been developed within the Bay by desorption of ^{226}Ra from freshwater fluvial sediment as it encountered salinity. However, due to the shape and estuarine nature of PPB, there are other possible sources of $^{210}Pb_{ex}$ to Central Bay which could explain the high value of I_{Pb}, and which could still lead to the CRS model being the most suitable model. These other sources include (1) $^{210}Pb_{ex}$ associated with sediment which may have been transported from shallow areas of the Bay and preferentially deposited or 'focussed' in the deeper areas of Central Bay; and (2) ^{210}Pb in Bass Strait water. From this analysis neither fallout nor catchment can be unequivocally identified as the dominant source of $^{210}Pb_{ex}$ to the Bay. Since it is not clear which dating model is appropriate, both models are considered below.

The CIC model

By assuming the concentration of ^{210}Pb in depositing sediment to be constant, the CIC model allows the segments of different slope to be analysed piece-wise, with each segment corresponding to a period of constant sedimentation, and inflexions corresponding to instantaneous shifts in sedimentation rate. All sediment samples from Central Bay show a similar layer of constant ^{210}Pb activity in the surface 2-3 cm (Figure 6). This is usually interpreted as being caused by sediment mixing which is rapid compared to the ^{210}Pb half-life (Krishnaswami *et al.*, 1971; Koide *et al.*, 1973), and this depth interval is not included in the regression analysis. A linear regression of $^{210}Pb_{ex}$ in the 3-20 cm depth interval of SC1 yields a sedimentation rate of 3.8 ±0.3 mm/y. The slope of the lower segment in Figure 6, corresponding to the depth region 20-45 cm, gives a sedimentation rate of 12 mm/y.

A similar calculation on data from the other Central Bay sediment samples, FS1 (3-20 cm depth) and SC3 (2-12 cm depth), yield rates of 4.3 ±0.3 and 4.5 ±0.4 mm/y. Again, the sedimentation rate was apparently much greater in deeper sediments. The rates derived for these three Central Bay profiles are indistinguishable given their associated uncertainties. Assuming the sedimentation rate is constant throughout Central Bay, the rates can be averaged to obtain a weighted mean, the weights being determined by the measurement uncertainty. The weighted mean is 4.1 ±0.2 mm/y. Based on the mean porosity (0.80) and dry sediment density (1.9 g/cm^3) in the 0-20 cm depth region, this rate is equivalent to 0.156 ±0.005 g/cm^2/y.

For the long core, LC3, the non-linearity of the log-linear plot is more pronounced. This plot shows 3 distinct regions of relatively constant $^{210}Pb_{ex}$ activity. Again, this profile can be explained by variable sedimentation rates, or by distinct regions of localised

rapid mixing, although in this case the effects appear to be more extreme, particularly in the upper 20 cm. It is possible that these regions of constant $^{210}Pb_{ex}$ activity were created by local artificial mixing (on a length scale of 10-20 cm) during collection and freezing. This core was much longer and narrower core than the shorter cores, and there was evidence that some distortion of the upper core profile occurred during freezing, particularly in the highly porous surficial sediments.

The Northern Bay core (SC2) shows two regions of different slope (Figure 7); a surface zone of apparent rapid mixing extending to a depth of about 10 cm, and a region (10-35 cm) where $^{210}Pb_{ex}$ decreases exponentially. The lower segment yields a sedimentation rate of 0.46 ±0.04 g/cm^2/y, or 3.6 ±0.3 mm/y based on the mean porosity (0.45) and density (2.3 g/cm^2) of sediment in this depth interval.

The CRS model

If the flux of ^{210}Pb to bottom sediments has remained constant, the age of sediment at depth z (t_z) can be estimated from

$$t_z = -\frac{1}{\lambda}\ln\left[1-\frac{I_z}{I}\right]$$

where I_z is the cumulative $^{210}Pb_{ex}$ inventory above depth *z* (Robbins, 1978). Using a value of 330 Bq/m^2 for total $^{210}Pb_{ex}$ inventory (I_{Pb}, section 3.2.4) the age of sediment in SC1 has been calculated as a function of depth, and plotted (Figure 8). Also plotted are the CIC model ages, which are significantly older than the CRS ages, particularly near the surface. The sedimentation rate derived from the CRS ages, given by the slope of the curve, is 8 mm/y. Application of this model to other Central Bay cores gives a similar sedimentation rate. This rate is a factor of 2 higher than that derived using the CIC model, and is not consistent with other estimates in this report (sections 3.3 and 3.4). Sediment mixing may be responsible for this high value.

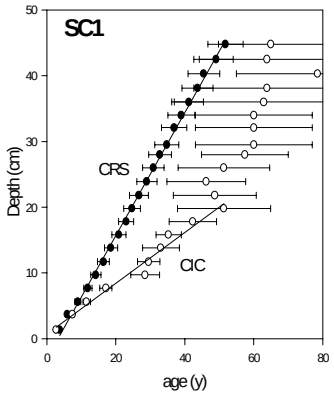

Figure 8. A comparison of sediment ages in core SC1 derived using the CIC and CRS models. The sedimentation rate derived from the CRS model is about twice the CIC rate.

3.2.4. Th-228

Th-228 (half-life 1.9 y) can be used to estimate sedimentation rates over a period of up to a decade (Koide *et al*., 1972; Huh *et al*., 1987). This nuclide is produced in the water column by the decay of ^{228}Ra (section 1.2). Settling particles scavenge ^{228}Th, leading to an excess of ^{228}Th activity ($^{228}Th_{ex}$) on the particles over its ^{228}Ra parent. The $^{228}Th_{ex}$ in the deposited sediment (given by the difference between the ^{228}Th and ^{228}Ra activities) can be used to determine sedimentation rates in a similar manner to $^{210}Pb_{ex}$.

Excess ^{228}Th is detectable to a depth of ~8-10 cm in SC1, FS1 and SC3. A regression of the log-linear plot of $^{228}Th_{ex}$ against depth yields a sedimentation rate of 12.9 ±2.8 mm/y in the top 10 cm of core SC1, and rates of 12.5 ±2.6 and 15.4 ±2.0 mm/y in the top 10 cm of FS1 and SC3. These values are not significantly different, and the weighted mean for Central Bay is 14.0 ±1.3 mm/y. This rate is a factor of three higher than the corresponding rate derived using $^{210}Pb_{ex}$. The difference could be due to an increase in the sedimentation rate over the last decade, or it could be due to sediment mixing. The $^{210}Pb_{ex}$ data is not consistent with an increased sedimentation rate in the upper 10 cm, indicating that mixing is the most likely explanation.

3.3. Sediment Accumulation and Mixing Rates

Bioturbation is reported to be a significant mixing process in PPB sediments (Bird *et al*., 1996), and will result in the transport of sediment grains and associated radionuclides to greater depths in the sediment. Depending on the rate of mixing, this process can increase the apparent sedimentation rate if the rate calculations are based solely on the reduction of ^{210}Pb activity at depth by radioactive decay (Robbins, 1978). If mixing is occurring in PPB sediments, the sedimentation rates derived above are 'apparent' rates only, and are upper estimates.

The effect of sediment accumulation and mixing on the depth profile of tracers in sediments has been modelled by Christensen (1982) using a one-dimensional advection-diffusion-decay equation, i.e.

$$\frac{\partial(\rho_w c)}{\partial t} = \frac{\partial}{\partial z}\left(K \frac{\partial(\rho_w c)}{\partial z} \right) - S \frac{\partial(p_w c)}{\partial z} - \lambda \rho_w c$$

where K is the sediment mixing coefficient (cm^2/y), S is the sediment accumulation rate (cm/y), λ is the decay constant of the tracer (y^{-1}), ρ_ω is the bulk density of the sediment (g/cm^3 wet sediment), and c is the activity concentration (mBq/g) at depth z (cm). The well known steady state solution to this equation is

$$A = A_0 e^{-bx}$$

where

$$b = \frac{S - \sqrt{\left(S^2 + 4\lambda K\right)}}{2K} \qquad (2)$$

and A (given by $\rho_w c$) refers to the activity distribution in mBq/cm^3 of the tracer in the bulk sediment at depth z, and A_0 is the activity at $z = 0$. The values of b are determined as in the previous section, from the least squares linear regression of the log-linear plot of the tracer against depth. Here the sediment bulk density is assumed to be constant, which is approximated in the top 40-50 cm of Central PPB sediments. Rearranging equation (2) gives,

$$S = \lambda/b - Kb$$

and

$$K = \lambda/b^2 - S/b. \qquad (3)$$

Hunter (pers. comm., 1994) showed that if the depth distribution of two tracers with different half-lives were known, the values of S and K could be derived. The half-lives of ^{210}Pb and ^{228}Th differ by a factor of about 12, and excess activities of both are present in the top 10 cm of Central Bay sediment. Under the assumption of constant sedimentation and mixing in the top 10 cm, S is determined from

$$S = \left(\frac{\lambda_{Pb}}{b_{Pb}^2} - \frac{\lambda_{Th}}{b_{Th}^2}\right) \Big/ \left(\frac{1}{b_{Pb}} - \frac{1}{b_{Th}}\right) \qquad (4)$$

where the subscripts Pb and Th denote ^{210}Pb and ^{228}Th. Weighted means of b_{Pb} and b_{Th} are derived from the three Central Bay profiles, and are 0.076 ±0.004 and 0.259 ±0.026 cm^{-1} respectively. From equation (4), S is calculated to be 0.01 ±0.9 mm/y. The sedimentation rate in Central Bay is therefore <0.9 mm/y. If we constrain S to be positive, the sedimentation rate can be expressed as 0.45 ±0.45 mm/y, and from equation (3) the corresponding value of K is 490 ±50 mm^2/y.

The positive value of K shows that mixing is occurring in the upper 10 cm of bottom sediments. Given that the slope of the $^{210}Pb_{ex}$ linear regressions in Figure 6 is constant to a depth of 20 cm for SC1 and FS1, and 12 cm for SC3, it is likely that S and K are constant to these depths. The changes in slope at around 20 cm may be due to different rates of mixing below this depth, with the increasingly shallow slope suggesting mixing rates may be even more rapid in deeper sediments. The depth of mixing indicated by the $^{210}Pb_{ex}$ distribution is >45 cm for the short cores, and may be as high as 70 cm in LC3. This mixing depth is consistent with the ^{228}Ra deficiency profile in LC3, which provides evidence for the bioturbation of sediments at depths of up 60 cm in Central Bay (see section 4.2.4).

3.4. The Depositional Rate of Suspended Particles

3.4.1. Water column residence time of ^{228}Th

Thorium isotopes can be used to estimate particle removal rates and settling rates in oceans and estuaries (e.g. Broecker *et al*., 1973; Li *et al*., 1979), allowing the determination of the flux of particles to the sea floor. This technique offers an independent estimate of the sedimentation rate, as well as giving an estimate of the water column residence time of particles. The disadvantages of this technique are (1) it cannot quantify how much of the sediment flux is resuspended sediment, and so the sedimentation rate estimate is an upper limit, and (2) the sedimentation rate estimate applies to a time period of just a few weeks prior to sampling.

The technique utilises the particle reactive nature of thorium, and assumes steady state between the *in situ* production of thorium in the water column by its soluble parent, and its subsequent removal. The removal processes are radioactive decay, and the adsorption of Th onto suspended particles followed by their subsequent deposition onto the sea floor. The relative activities of parent and daughter nuclide give a measure of the residence time of the Th daughter in the water column, and hence the residence time of suspended particles in the water column. Broecker *et al*. (1973) showed that the mean life-time of ^{228}Th with respect to removal from the water column, τ_{Th}, could be derived from

$$\tau_{Th} = [R/(1-R)]1/^{228}\lambda_{Th}$$

where R is the daughter/parent activity ratio, $^{228}Th_{a+d}/^{228}Ra_w$, and $^{228}\lambda_{Th}$ is the decay constant of ^{228}Th. $^{228}Ra_w$ in this ratio is the dissolved ^{228}Ra activity in the water column, and $^{228}Th_{a+d}$ is the combined activity of dissolved ^{228}Th and ^{228}Th adsorbed to suspended particles.

In this study, water samples were not filtered, and suspended particles were included in the analysis of the 'total' sample. The analysis procedure included an acid leach, and so the measured Ra and Th activities of the water sample include not only dissolved activity, but also a particle-bound component. The fraction of particle-bound ^{228}Ra activity in the water column is small (<1% of the total), and the measured ^{228}Ra activities are essentially dissolved. However, a large fraction of Th isotope activity in the water column is particle-bound. This fraction will include not only Th sorbed to the surface of particles, but also Th leached from the mineral phases that make up the particles.

The ^{228}Th in this leached phase will have been generated within the mineral lattice, and since the determination of τ_{Th} requires a measure of just the ^{228}Th generated in the water column ($^{228}Th_{a+d}$), the leached ^{228}Th activity must be deducted from the measured ^{228}Th activity. This is done by deducting an activity equal to the measured ^{232}Th activity to give $^{228}Th_{a+d}$, since the ^{232}Th and ^{228}Th activities in the mineral phases will be approximately equal, and the dissolved ^{232}Th activity to is likely to be negligible, meaning that virtually all the measured contribution of ^{232}Th activity can be assumed to come from the mineral lattice of the sediment.

The values of $^{228}Th_{a+d}$, R, and τ_{Th} are given in Table 1. Because τ_{Th} measures the residence time of ^{228}Th in the water column, it includes both the time taken for scavenging of dissolved ^{228}Th by suspended particles, and the time for the removal of these particles by settling. Thus the values of τ_{Th} derived from this work represent an upper limit for the particle residence time in the water column. In order to estimate the relative magnitudes of the ^{228}Th scavenging time and particle residence time, measurements of dissolved and particulate ^{228}Th were made on two PPB water samples collected June 1997. These samples had similar levels of SS to the February 1996 samples. The dissolved (<0.45 μm) ^{228}Th activity in these samples was found to be only about 10% of the total water sample. Based on these measurements, the mean time for scavenging of Th is ~1 day, which is short, compared to the time for particle removal.

The values of τ_{Th} range from 8 to 43 days, with most values lying between 8 and 16 days. Apart from the bottom water sample from site 2, the values of τ_{Th} at each site are not significantly different from each other, and do not show a trend with depth. In a water column with no vertical mixing, sinking particles would show a monotonic increase of $^{228}Th_{a+d}$, and hence $\tau_{Th,}$ with depth. The time taken for a particle to settle through the water column could then be estimated from the difference between τ_{Th} at the surface and the base of the water column. The lack of any trend in τ_{Th} with depth at most sites in PPB suggests that the time scale for vertical mixing at these sites is short compared to the time taken for particles to settle through the water column. This observation is consistent with the conclusion drawn in section 4.1.

The bottom water sample from site 2 (Hobson's Bay) has high values of both τ_{Th} and C_p. This may be due to an accumulation of settling particles near the bottom, or repeated resuspension of recently deposited sediment. Since site 2 was the shallowest site sampled (13 m depth), the rate of sediment resuspension by wave or current action is likely to be greater than at deeper sites.

3.4.2. The flux of particles to the Bay floor

Knowledge of τ_{Th} allows an estimate of the flux of particulates (F_p) to the bottom sediments. It is assumed here are that steady state exists with respect to input and removal of particles in the Bay, and that Th removal from the water column is due entirely to the settling of suspended particles onto the floor of the Bay.

Both these assumptions are reasonable. No significant change in the rate of sediment input into the Bay occurred over the time scale relevant to the estimate of τ_{Th} (20-30 days), and the fraction of suspended particles lost by advection to Bass Strait is negligible compared to losses by sedimentation. This is because the mean residence time of particles in the water column (~10 d, see below) is much less than the residence time of water in the Bay (~270 days, Walker *et al*., 1992).

A further check on the efficiency of the removal of dissolved ^{228}Th and its deposition can be made by comparing the depositional flux required to sustain the $^{228}Th_{ex}$ inventory (F_{Th}) in bottom sediments with the production rate of ^{228}Th in the water column. If all

the ^{228}Th produced in the water column is deposited onto the sea floor directly below, then

$$F_{Th} = {}^{228}\lambda_{Th} c_{Ra} H$$

where H is the water column depth, c_{Ra} is the water column concentration of ^{228}Ra. The $^{228}Th_{ex}$ inventory (I_{Th}) is calculated following the same procedure as for I_{Pb} (equation (1)). The values of I_{Th} in three Central Bay sediment samples (SC1, FS1, SC3) are 30 ±5, 48 ±8 and 35 ±6 mBq/cm^2, and the fluxes required to sustain these inventories (given by $^{228}\lambda I_{Th}$) are 10.9 ±1.8, 17.4 ±2.9 and 12.7 ±1.8 mBq/cm^2/y. These fluxes compare well with the average Central Bay water column production rate of ^{228}Th (15.5 ±1.4 mBq/cm^2/y), indicating that the efficiency of deposition of ^{228}Th is high. This comparison also provides further evidence that our sampling procedures recovered the surficial sediment.

The flux of particulates to the Bay floor (F_p) can be estimated by

$$F_p = \frac{C_p H}{\tau_p} \qquad (5)$$

where C_p is the suspended particulate concentration of the water column, and τ_p is the particle residence time, which is estimated by deducting the ^{228}Th scavenging time (~1 day) from τ_{Th}. Because C_p and τ_p are relatively constant with depth, mean values of these parameters have been used in equation (5) to derive F_p at each site (Table 7). At site 2, only the surface and mid-depth samples have been averaged, and so F_p at this site only applies to the top half of the water column. The mean of the values of F_p at the two Central Bay sites (1 and 3) is 0.18 ±0.03 g/cm^2/y. This is close to the fluxes determined using sediment traps in the Central Bay region (0.12 g/cm^2/y; You *et. al*, 1996).

The fluxes derived above only correspond to a 2-3 week period in February 1996, and are dependent on the values of C_p at the time of sampling. However, the average suspended solids concentration in the Central Bay region over the last 7 years (2.5 mg/L, A. Longmore, pers. comm.) is close to the mean of our measurements of C_p in Central Bay (sites 1 and 3) in February 1996 (2.1 mg/L). Thus, F_p probably represents a good estimate of the long-term average flux of particles onto the floor of Central Bay.

The value of F_p at site 2 (0.083 ±0.25 g/cm^2/y) is much lower than the sediment trap estimates (7.0 g/cm^2/y; You et. al, 1996). This is probably due to the fact that F_p at this site is based on the C_p content of the upper half of the water column, whereas the sediment traps were situated less than 2 m from the sea floor. It would appear therefore, that unless there was an unusually high influx of sediment into the Bay at the time the traps were in place, the high sediment trap estimates are due to local resuspension of bottom sediment.

Table 7. Mean suspended sediment concentrations ($C_{p,}$), ^{228}Th residence time (τ), particle flux (F_p), and normalised particle flux (r_p).

site	H (m)	C_p (mg/L)	$^{**}\tau_p$	F_p (g/cm^2/y)	r_p (g/cm^2/y)
1	25	2.3	10.6 ±2.1	0.20 ±0.04	0.16 ±0.03
2*	13	2.9	12.2 ±4.0	0.11 ±0.03	0.09 ±0.02
3	25	1.8	9.6 ±2.8	0.17 ±0.04	0.14 ±0.04
4	19	2.1	13.2 ±3.2	0.11 ±0.02	0.09 ±0.02
5	14	2.9	9.0 ±1.3	0.16 ±0.02	0.13 ±0.02

* The bottom water sample is not included in the determination of the mean values of C_p and τ_p at site 2.
** A mean ^{228}Th scavenging time of 1 day has been assumed, and deducted from τ_{Th} to give τ_p (see text).

3.4.3. Conversion to sedimentation rate

When using these fluxes to estimate sedimentation rates, differences in the composition of SS and bottom sediment must be considered. The ^{232}Th content of sediment has often been used to normalise the concentrations of radionuclides in sediment, thus correcting for variable content of low activity material, such as organic matter. The ^{232}Th of SS in February 1996 was about 20% lower than the bottom sediment, perhaps indicating a higher organic matter content of SS. This organic matter is presumably decomposed or recycled when it is deposited (Wilson *et al.*, 1993). Thus, F_p must be reduced by 20% if it is to be used as an estimate of the apparent sedimentation rate. This reduction gives a mean normalised particle flux (r_p) of 0.145 ±0.022 g/cm^2/y in Central Bay region, equivalent to 3.8 ±0.6 mm/y using surficial Central Bay sediment porosity and density values. The value of r_p at each site is given in Table 7.

Again, it is noted that r_p is not necessarily the rate of sediment accumulation, because it includes resuspended sediment. As an estimate of net sedimentation rate it is therefore an upper limit, and the true rate must be <0.17 g/cm^2/y, or <4.4 mm/y. Although r_p in the Central Bay agrees reasonably well with data obtained from sediment traps, the sedimentation rate calculated here (in mm/y) differs by a factor of about three from that reported in the Port Phillip Bay Final Report (Harris *et al.*, 1996). This is due to the use of different sediment density and porosity values to convert sediment fluxes to a linear sedimentation rate.

3.5. Summary of Sedimentation Results

The sedimentation study results are summarised in Table 8. The tightest constraint on the sedimentation rate is obtained from the combined bottom sediment depth profiles of ^{210}Pb$_{ex}$ and ^{228}Th$_{ex}$. These tracers constrain the sedimentation rate to be <0.9 mm/y, or <0.034 g/cm^2/y. They also show that sediments in Central and Northern PPB are certainly mixed to a depth of 10 cm, and are probably mixed to a depth of least 20 cm.

This mixing means that the sedimentation rate derived directly from the distribution of $^{210}Pb_{ex}$ in cores (4.3 mm/y in Central Bay) is an upper estimate.

A measure of the rate of suspended particle deposition was derived from the production/removal equilibria of ^{228}Th in the water column. The mean residence time of particles in the water column of Central PPB was found to be about 10 days at the time of sampling (February 1996). This process yielded an equivalent sediment flux of 0.145 g/cm^2/y to the floor of Central PPB. However, this estimate only provides an upper limit to the sedimentation rate, due to the likely presence of resuspended sediment in the water column.

Harris *et al*. (1996) estimated the total sediment input to the PPB to be 85,000 tonnes/y over the period 1992-95. If this sediment is assumed to be deposited uniformly over the Bay (area 1950 km^2), the corresponding sedimentation rate is 0.004 g/cm^2/y. However, $^{210}Pb_{ex}$ inventory calculations indicate that focussing of sediment may be occurring in the deeper regions of PPB. These deeper regions (>15 m) cover about half of the surface area of the Bay, and contain most of the silt and clay sediments in the Bay. If all the SS delivered to the Bay is considered to preferentially deposited in these deeper areas, the calculated sedimentation rate in these areas is doubled, to 0.008 g/cm^2/y. This rate is well within our best estimate of the sediment accumulation rate in Central Bay (<0.034 g/cm^2/y), which in turn is much lower than the depositional flux of particles to the Bay floor (0.15 g/cm^2/y). Such a high depositional flux indicates that most (>80%) of the suspended sediment in PPB is resuspended bottom sediment.

Table 8. Summary of sedimentation results. Units are mm/y (top value) and g/cm^2/y (brackets).

Region	sites	Method		
		$^{210}Pb_{ex\ core\ profile}$	2 tracer core profile, $^{228}Th_{ex}$ and $^{210}Pbex$	Particle flux from water column production of $^{228}Th_{ex}$
Central	1, 3	<4.3 (<0.163)	<0.9 (<0.034)	<4.4 (<0.17)
Northern	2	<3.9 (<0.46)		<1.7 (<0.11)

4. WATER COLUMN MIXING PROCESSES

4.1. Vertical mixing

4.1.1. Source of short-lived Ra isotopes to PPB

The sources of dissolved Ra to estuaries include seawater, groundwater, Ra dissolved in river water, Ra desorbed from riverine suspended sediment, and diffusion of Ra from bottom sediments. For the longest-lived Ra isotope, ^{226}Ra, all sources contribute significantly to the standing crop of ^{226}Ra in PPB. However, the input of short-lived isotopes (^{224}Ra, ^{223}Ra, ^{228}Ra), from rivers, seawater and groundwater is insignificant compared to their flux from bottom sediments (see discussion in section 4.3). There is some generation of ^{224}Ra by its parent (^{228}Th) in the water column, but based on typical water column SS concentrations, this is <10% of the total water column activity of ^{224}Ra. Consequently, more than 90% of the water column activity of ^{224}Ra is estimated to originate as a continuous flux from bottom sediments.

Once Ra has diffused into the water column, it behaves essentially as a conservative tracer of water movement. And because the water column content of Th is very low, Ra isotopes are essentially unsupported in the water column. Thus the water column activities of Ra isotopes in combination with their radioactive decay rates can be used to yield information on water column mixing rates. The shortest-lived isotope, ^{224}Ra (half-life 3.7 d) is especially useful for this. Any ^{224}Ra activity the water column in excess of ^{228}Th activity must have been generated and released from bottom sediments within a time frame of days-weeks. If vertical mixing of the water column is occurring on a time scale similar to, or longer than the ^{224}Ra half-life, a vertical ^{224}Ra concentration gradient will arise.

4.1.2. Water column activities of ^{224}Ra

The water column activities of ^{226}Ra, ^{228}Ra and ^{224}Ra are given in Table 1. The relative uncertainties of ^{223}Ra measurements were high, and its activities are not reported. Included in Table 1 is the unsupported water column activity of ^{224}Ra ($^{224}Ra_{ex}$), given by the difference between the water column activity of ^{224}Ra and its parent ^{228}Th; $^{224}Ra_{ex}$ is therefore a measure of ^{224}Ra activity which has diffused from bottom sediments.

For ^{226}Ra and ^{228}Ra there is no significant difference in concentration between the sites. Nor is there any trend with depth. However, $^{224}Ra_{ex}$ shows some variation between sites, with the highest concentrations occurring at site 2. The $^{224}Ra_{ex}$ activities of the surface, mid-depth and bottom samples are indistinguishable at sites 2, 4 and 5. This result indicates that vertical mixing of the water column is occurring on a time short compared to the half-life of ^{224}Ra. When the measurement uncertainties are considered, this time scale corresponds to less than 1.5 days for mixing between surface and bottom water.

In the Central Bay region, however, a vertical $^{224}Ra_{ex}$ gradient is present at site 1, and possibly at site 3. At site 1, the bottom sample has the highest $^{224}Ra_{ex}$ activity (10.2 ±1.2 mBq/L). This activity is about three times that of the mid-depth and surface samples at this site. The concentration profile at this site indicates that the top half of the water column had been rapidly mixed, but that mixing between bottom water and water above it had been restricted. This observation indicates the presence of a pycnocline between 12 and 24 m depth. Unfortunately, the salinity/temperature/ density probe failed to function properly during sample collection, and the presence of the pycnocline could not be confirmed. However, salinity and temperature gradients are common in the Central Bay area in summer (A. Longmore, pers. comm.). Determination of the mixing rate of bottom water and water above it is not warranted without time-series measurements, and/or a more highly resolved depth distribution of ^{224}Ra than was obtained from this study. Nevertheless, the fact that $^{224}Ra_{ex}$ concentration in surface and mid-depth water at site 1 is similar to other regions of PPB suggests that the pycnocline had been established only recently, else water had been recently advected to Central Bay from a region of the Bay where the water column was well-mixed.

It is interesting to note that the bottom water at site 3 had a much lower $^{224}Ra_{ex}$ concentration than site 1, despite the close proximity of the sites, and similar water column depths. This could be due to strong winds (up to 20 knots) which occurred on February 28, the day separating sampling at site 1 (February 27) and site 3 (February 29). These winds may have been strong enough to mix bottom and surface water in the previously stratified Central Bay.

4.2. Surface Water-Porewater Exchange

4.2.1. The flux of ^{224}Ra from bottom sediments

It has been shown that Ra isotope data can yield information on the extent of surface water-porewater exchange in the Bega estuary (Webster *et al*. 1994; Hancock and Murray 1996). The characteristics of PPB make it ideal for the study of sediment-water interactions using Ra, because nearly all the short-lived Ra isotopes in the PPB water column have originated from bottom sediments, where they are continually produced by insoluble Th parents (see section 4.1.1). The most important removal processes of Ra from the water column will include radioactive decay, uptake by suspended biota and deposition to the Bay floor, and advection too Bass Strait. The water column residence time of suspended particles (10 d, section 3.4) is long compared to the ^{224}Ra half-life, indicating that biota are not likely to be significant removal pathway for ^{224}Ra. The residence time of water in PPB is estimated to be at least 230 days (see section 4.3 below), and so the fraction of Ra lost to Bass Strait will only be significant for the longer lived isotopes, ^{226}Ra and ^{228}Ra. Thus if steady state is assumed, the flux of Ra from bottom sediments will equal the rate of loss of Ra from the water column by radioactive decay, and the total flux of ^{224}Ra from bottom sediments ($^{224}F_s$) can be estimated from

$$^{224}F_s = {}^{224}\lambda_{Ra}\,\bar{c}_{wc}\,H \qquad (6)$$

where c_{wc} is the mean water column ^{224}Ra concentration, calculated by averaging the surface, mid and bottom water samples at each site, $^{224}\lambda_{Ra}$ is the ^{224}Ra decay constant, and H is the depth of the water column at that site. The values of $^{224}F_s$ at each site are given in Table 9.

4.2.2. Diffusion of ^{224}Ra

Two processes are likely to control the flux of dissolved Ra from bottom sediments into the water column. These are molecular diffusion of Ra across the sediment-water interface, and the physical exchange of surface water and porewater due to surface water currents and bio-irrigation by animals in the sediment (Nicholson *et al*., 1996). A diffusive flux of Ra from sediment to water column occurs because the Ra concentration in bottom sediment porewater is much higher than the overlying surface water. This flux can be estimated by assuming that diffusion of Ra across the sediment-water interface is controlled by one-dimensional diffusion of ion-exchangeable Ra within bottom sediments. Because Ra isotopes are continuously created within the sediments, and are continually exchanging between porewater and ion-exchange sites on the sediment, the total amount of ion-exchangeable Ra contained within the sediments must be considered. Hence

$$C_e = \phi c_{pw} + C_s$$

where ϕ is the sediment porosity, C_e is the total concentration of ion-exchangeable Ra in sediment (dissolved + adsorbed), C_s is the component of C_e adsorbed to sediment grains, and c_{pw} is the Ra concentration in porewater. Both C_e and C_s have units of activity/unit volume of sediment; c_{pw} has units of activity/unit volume of porewater. Thus ϕc_{pw} is the concentration of dissolved Ra expressed as activity/unit volume of sediment.

The distribution of Ra between sediment and porewater can be described by a desorption function Θ (Webster *et al*., 1995). In essence, Θ represents the fraction of total ion-exchangeable Ra in sediments that exists in porewater, ie.

$$\phi c_{\mathrm{pw}} = \Theta C_{\mathrm{e}} \qquad (7)$$

The equation describing the rate of change with time of ion-exchangeable Ra within sediments can be written as

$$\frac{\partial C_e}{\partial t} = -\frac{\partial F_d}{\partial z} - \lambda C_e + \gamma \qquad (8)$$

where z is the vertical coordinate (positive upwards), γ is the rate of production of ion-exchangeable Ra, and F_d is the diffusive flux of Ra through the sediment, given by

$$F_d = -\phi D_s \frac{\partial c_{pw}}{\partial z} \quad \text{,(Ullman and Aller, 1982).} \qquad (9)$$

Here D_s is the diffusion coefficient of Ra in sediment, and is estimated from the relationship

$$D_s = \phi^2 D_0$$

when $\phi > 0.7$; D_0 is the diffusivity of Ra in water (7.45×10^{-6} cm^2/s at 18° C; Li and Gregory, 1974). The temperature of bottom water at the time of sampling was ~18° C, and based on a porosity of 0.82 in surficial in Central Bay sediments, D_s is 5.0×10^{-6} cm^2/s. Using equations (6) and (8) we obtain

$$F_d = \Theta D_s \frac{\partial C_e}{\partial z} \tag{10}$$

By introducing D' as the effective diffusivity for C_e, such that

$$D' = \Theta D_s \tag{11}$$

equation (8) becomes

$$\frac{\partial C_e}{\partial t} = D' \frac{\partial^2 C_e}{\partial z^2} - \lambda C_e + \gamma$$

At steady state $\frac{\partial C_e}{\partial t} = 0$, and solving for C_e gives

$$C_e \sim A e \sqrt{\frac{-\lambda z}{D'}} + \frac{\gamma}{\lambda} \tag{12}$$

where A is a constant to be determined by the boundary conditions at the sediment-water interface. In the derivation of (12) it has been assumed that as $z \to -\infty, \frac{\partial C_e}{\partial t} \to 0$. At the sediment-water interface (z = 0) we have $C_0 = A + \frac{\gamma}{\lambda}$. Neglecting the presence of a significant concentration gradient on the water side of the sediment-water interface (a good assumption), C_0 should match the Ra concentration in the water column. If this is the case, C_0 is small compared to C_e, and $A \sim -\frac{\gamma}{\lambda}$. From equations (10) and (12) the diffusive flux of Ra across the sediment-water interface is

$$F_d = AD' \sqrt{\frac{\lambda}{D'}}$$

$$\approx C_{-\infty} \sqrt{\lambda D'} \tag{13}$$

Because of the short half-life of ^{224}Ra, the length scale of variation of C_e due to diffusion (given by $1/\sqrt{\lambda D'}$) is also short, and $C_{-\infty}$ (C_e at $z = -\infty$) is attained at a depth of a few mm. The method for estimating $C_{-\infty}$ is outlined in Webster *et al*., (1995). Its value was determined from desorption experiments conducted on sediment collected from site 3, and found to be 7.5 mBq/cm^3. The value of Θ for ^{224}Ra (0.024) was then derived using this value of $C_{-\infty}$, and the ^{224}Ra porewater concentration of the same sediment (c_{pw} = 0.18 mBq/cm^3). Substituting these values into equations (11) and (13), gives a diffusive ^{224}Ra flux ($^{224}F_d$) of 3.8 x 10^{-6} mBq/cm^2/s at the sediment-water interface. This is 24% of the total ^{224}Ra flux ($^{224}F_s$) from bottom sediments at site 3, derived using equation (6).

Nicholson *et al*. (1996) calculated flux enhancement factors for some solutes in PPB sediments from benthic chambers measurements. These factors give a measure of the enhancement of the flux of a solute due to non-diffusive processes such as bioirrigation, and are derived from the ratio of the measured flux of a solute across the sediment-water interface to the flux attributed solely to molecular diffusion. The values ranged from 0.3 for NO_x to 8.0 for Si. From $^{224}F_d$ and $^{224}F_s$, the ^{224}Ra flux enhancement factor in Central Bay is 4.2, which lies in the middle of the range of factors for other solutes.

4.2.3. Rate of porewater exchange

As noted above, molecular diffusion of ^{224}Ra can account for only 24% of $^{224}F_s$. Consequently, non-diffusive transport must account for at least the remaining 76%. Based on benthic chamber experiments (Nicholson *et al*., 1996; Berelson *et al*., 1994), this transport appears to be largely due to the physical exchange of surface water and porewater. Thus, the flux of water (F_w) crossing the sediment-water interface can be estimated from

$$F_w = \left({}^{224}F_s - {}^{224}F_d\right) / \left({}^{224}c_{pw} - {}^{224}\bar{c}_{wc}\right)$$

Here c_{pw} represents the ^{224}Ra concentration of porewater advected across the sediment-water interface. Our measured value of c_{pw} is an average ^{224}Ra porewater concentration in the top 10 cm of Central Bay sediment (0.18 mBq/L). Since it is possible that porewater may have been transported from depths greater than 10 cm, there is some uncertainty in our calculated value of F_w. However, assuming c_{pw} to be representative of advected porewater, F_w at site 3 is 6.8 x 10^{-5} cm^3/cm^2/s. Over a year, this flux amounts to a significant fraction of the PPB water column. For example, if our calculated value of F_w is typical of the whole of PPB, a volume of water approximately equal to 1.7 times the volume of PPB is advected across the sediment-water interface each year.

Berelson *et al*. (1994) determined the flux of Cs crossing the sediment-water interface in benthic chambers deployed on the floor of PPB. The Cs was injected to the chamber, and its loss monitored. They concluded that the loss of Cs from the chamber was much greater than could be accounted for by molecular diffusion, indicating that non-diffusive processes such as irrigational advective transport between sediment porewater and the overlying water were primarily responsible for the Cs loss. Using the rate of loss of Cs

from each chamber and the corresponding initial Cs concentration, we calculate the flux of water across the sediment-water interface in chambers from Central Bay to range from 7.2 x 10^{-5} to 34 x 10^{-5} $cm^3/cm^2/s$. The value of F_w at site 3 (derived above using Ra data) lies close to the lower end of this range, and provides independent evidence for the presence of advective exchange of surface water and porewater. The agreement between the ^{224}Ra flux technique and the benthic chamber techniques is reasonable, given the uncertainty in c_{pw}, and considering the greater statistical variation associated with spot measurements using chambers, compared to Ra-derived porewater fluxes which have been averaged over a much larger area.

Table 9. Summary of parameters used to derive $^{224}F_s$

site	water column depth (m)	c_{wc} (mean water column $^{224}Ra_{ex}$) (mBq/L)	$^{224}F_s$ (x 10^{-5} $mBq/cm^2/s$)
1	25	6.1	3.3
2	13	5.2	1.5
3	25	3.0	1.6
4	19	3.3	1.4
5	15	2.8	0.9

4.2.4. Depth of bioturbation

The flux of dissolved Ra from bottom sediments leaves a temporary deficiency of ^{228}Ra activity with respect to its parent ^{232}Th. Figure 9 (a) shows a plot of the ^{228}Ra/^{232}Th activity ratio (AR) against depth for LC3. The ^{228}Ra/^{232}Th AR increases from about 0.7 at the surface of the core, to a value consistent with unity at a depth of about 70 cm. If bottom sediments were a closed system, with no net gain or loss of radionuclides, nuclides of the ^{232}Th-series would reach secular equilibrium within 30 years. Their activities would then be the same, and the AR of any two nuclides in the series would be equal to one. The fact that ^{228}Ra/^{232}Th AR is <1 in the top part of the sediment profile indicates ^{228}Ra is continually being lost from this region.

As noted in the previous section, the length scale of diffusion for Ra is given by $1/\sqrt{\lambda D'}$ (equation (12)). Using the value of D' derived above, the length scale for ^{228}Ra diffusion is calculated to be about 6 cm. Because ^{228}Ra deficiency occurs to a depth of 60-65 cm, it is clear that non-diffusive processes have played an important role in exporting radium from deeper sediments. The processes most likely to be responsible for this export are bioirrigation (water exchange) and/or bioturbation (sediment mixing). Burrowing shrimps and worms can aid sediment redistribution and water movement through sediments by creating tunnels, and these animals are reported to be active in PPB sediments at a depth of 40 cm, and perhaps deeper (Bird *et al.*, 1996). For the ^{228}Ra deficiency to be maintained, these irrigation and/or mixing processes must be occurring on a time scale equal to or shorter than the ^{228}Ra half-life (6 years). There is strong

evidence for bioturbation at depths of 50 cm or more from the presence of significant concentrations of $^{210}Pb_{ex}$ in the depth interval 20-72 cm (Figure 6). Based on our upper estimate of sedimentation (0.9 mm/y), $^{210}Pb_{ex}$ would not be detectable below 15 cm without sediment mixing to aid its transport to greater depths.

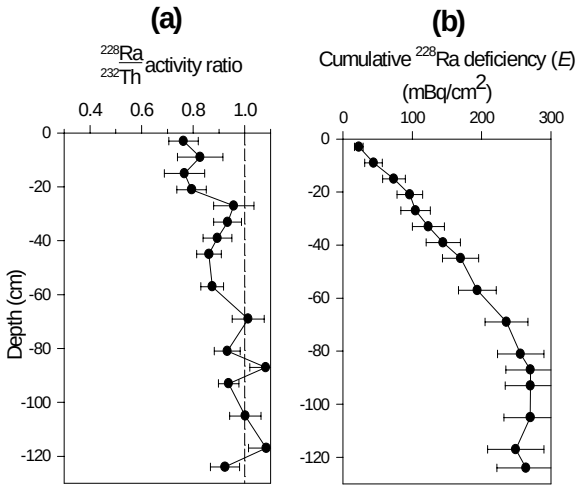

Figure 9. The LC3 depth profile of (a) the $^{228}Ra/^{232}Th$ activity ratio, and (b) cumulative ^{228}Ra deficiency.

4.3. Residence Time of Water in the Bay

4.3.1. Input and output fluxes of ^{228}Ra

The standing crop of dissolved Ra in the PPB water column can be expressed as a balance between input and output fluxes, i.e.

$$F_s + F_{riv} + F_{gw} = H\lambda_{Ra} c_{wc} + R_{ad} + R_{bio} \qquad (14)$$

where the *F* terms on the left side of the equation are input fluxes, with subscripts denoting Ra flux from bottom sediments (s), riverine inputs (riv), and groundwater (gw). The right side includes output or loss terms. These include a decay term, $H\lambda c_{wc}$, where *H* is the average water column depth of the Bay, λ_{Ra} is the Ra decay constant, and c_{wc} is the mean water column concentration of Ra in the Bay. Other loss terms include the removal of Ra by advection or mixing to Bass Strait (R_{ad}), and removal of Ra by biological uptake (R_{bio}). If the Ra concentration is relatively constant throughout the Bay, R_{ad} can be expressed as

$$R_{ad} = H \frac{(c_{wc} - c_{BS})}{t_w} \qquad (15)$$

where c_{BS} is the Ra concentration of Bass Straight water, and t_w is the mean residence time of water in the Bay. Equations (14) and (15) show that if the input and output Ra fluxes can be quantified, the residence of water in PPB can be determined.

The best isotope for this study is ^{228}Ra, because (1) it is shown below that the input of ^{228}Ra to PPB is dominated by a single quantifiable term, the flux from bottom sediments ($^{228}F_s$); (2) the ^{228}Ra concentration in PPB water is much greater than Bass Strait water, and (3) the concentration of ^{228}Ra in the PPB water column shows little variation throughout the Central and Northern Bay regions, which are the areas containing most of the PPB water. Thus PPB can be assumed to be a well-mixed box with respect to ^{228}Ra.

Because of its relatively long half-life, the ^{228}Ra decay term in equation (14) is small, and most of the ^{228}Ra in the PPB water column is eventually advected into Bass Straight. Consequently, the method used to estimate $^{224}F_s$ (section 5.1) cannot be used to estimate $^{228}F_s$. Instead, $^{228}F_s$ can be estimated by considering the integrated deficiency of ^{228}Ra (E) in bottom sediments with respect to its parent ^{232}Th (Thomson *et al*., 1975; Turekian *et al*., 1996). The causes of ^{228}Ra deficiency in bottom sediments have been described in the previous section, and its integrated activity is calculated from

$$E = \sum_{i=1}^{\infty} (^{232}C_i - ^{228}C_i) m_i$$

where $^{232}C_i$ and $^{228}C_i$ are the sediment concentrations of ^{232}Th and ^{228}Ra in depth section i, and m_i is the mass per unit area of that section. Assuming this deficiency is due only to losses of Ra to surface water, and that steady state applies, the flux of from bottom sediments required to sustain E is

$$^{228}F_s = {}^{228}\lambda_{\mathrm{Ra}}\, E \qquad (16)$$

where $^{228}\lambda_{\mathrm{Ra}}$ is the ^{228}Ra decay constant. A plot of cumulative E and depth in LC3 is shown in Figure 9(b). Where ^{232}Th and ^{228}Ra data are missing, the ^{228}Ra deficiency has been interpolated. Cumulative E reaches a maximum of about 265 ±37 mBq/cm^2 at a depth of about 80 cm. From equation (16), $^{228}F_s$ at site 3 is 32 ±4 mBq/cm^2/y.

The depth profile of the ^{228}Ra/^{232}Th AR in the two short cores from Central Bay (SC1 and SC3, Tables 2 and 4) is comparable with LC3, indicating that $^{228}F_s$ is relatively constant in this region of the Bay. The same treatment of the Northern Bay core (SC2) data yields 37 ±4 mBq/cm^2/y for $^{228}F_s$, which is also similar to the Central Bay value. Given the different physical characteristics of sediment in Northern PPB, and the shorter depth of sediment in which ^{228}Ra deficiency is present, this similarity is probably coincidental. A third measure of $^{228}F_s$ was obtained from a long core taken at site 4, in the Northern-Central Bay region (LC4). However, on this occasion the sediment was not sectioned. Instead a method requiring the measurement of Ra and Th in only two samples was used. The entire core was mixed and the value of E determined from the total mass of sediment, and the measured deficiency of ^{228}Ra in the mixture. Equilibrium between ^{232}Th and ^{228}Ra at the base of the core (1 m depth) was confirmed by measurement of a separate sample taken prior to mixing. The value of $^{228}F_s$ at this

site (34 ±8 mBq/cm^2/y) is indistinguishable from the Central Bay estimate, a result which is not surprising given the similarity in sediment type.

The similarity of these three measures of $^{228}F_s$ suggests that the flux of ^{228}Ra from bottom sediments is relatively constant at around 34 mBq/cm^2/y over a large proportion of the Bay. However the Bay-wide flux of ^{228}Ra is required to determine t_w, and no measure of $^{228}F_s$ was obtained around the edge of the Bay where sediments are coarser grained (Greilach *et al*., 1996), consisting mainly of sand and gravel (light shading, Figure 1). This region comprises about 25% of the area of the Bay, and the ^{232}Th concentrations of sediments in this region are likely to be lower than other areas of the Bay. Since ^{232}Th is the source of ^{228}Ra in sediment, it is probable that $^{228}F_s$ is also lower in this region. The implications of this lower flux for residence time calculations are considered in the following section (4.3.2).

Other ^{228}Ra input terms can be estimated from data supplied in Harris *et al*. (1996). The total inflow into the Bay from rivers and creeks is estimated to be about 44 m^3/s. The dissolved ^{228}Ra concentration in fresh surface water is usually low (<1 mBq/L), and a riverine Bay-wide flux of <0.07 mBq/cm^2/y is expected. Sediment input to the Bay is estimated to be 85,000 t/y. Assuming that ^{228}Ra and ^{232}Th activities of the incoming freshwater sediment are in secular equilibrium, and that the desorptive loss of ^{228}Ra from this sediment is similar to that observed in surficial sediments in the Central Bay (~40% of the ^{232}Th activity), then the extent of desorption of ^{228}Ra from this sediment as it encounters saline water is about 22 mBq/g. This loss amounts to a Bay-wide desorption flux of 0.10 mBq/cm^2/y. These two components of F_{riv} (dissolved and desorbed) amount to 0.2 mBq/cm^2/y.

The groundwater flow into the Bay is estimated to be greater than 1.7 m^3/s (Otto, 1992). The Ra content of this water is not known, and it will depend on numerous factors such as salinity and composition of the host soil/rock. Based on concentrations reported in the literature, groundwater ^{228}Ra concentrations greater than 300 mBq/L are uncommon (e.g. Osmond and Cowart, 1992; Martin and Akber, 1996). If 300 mBq/L is taken as an upper limit for groundwater entering PPB, and an input volume of 2 m^3/s is used, the value of F_{gw} will not exceed 1.0 mBq/cm^2/y. Thus the combined riverine and groundwater flux of ^{228}Ra is probably no greater than 4% of the bottom sediment flux, and to a first approximation can be ignored.

The rate of removal of Ra from the water column by biological uptake is also unknown, but other estuarine and near-shore studies have concluded that this uptake is insignificant (Hancock and Murray, 1996; Kasemsupaya *et al*., 1993). In any case, if the main pathway for biological removal of Ra from the water column is by uptake by suspended biota, followed by deposition onto the Bay floor, biological removal does not need to be considered separately as a removal process. This is because the flux of biologically-bound Ra to bottom sediments will reduce the ^{228}Ra deficiency therein. Consequently, this process has already been incorporated into left side of equation (14) as a negative component of $^{228}F_s$.

4.3.2. Calculation of water residence time

By neglecting F_{riv}, F_{gw} and R_{bio}, and rearranging equations (14) and (15), the mean residence time of PPB water can be estimated from

$$t_w = \frac{H(c_{wc} - c_{BS})}{(F_s - H^{228}\lambda_{Ra}c_{wc})} \qquad (17)$$

The ^{228}Ra concentration of Bass Strait water near the entrance of PPB was measured in June 1997. Two samples were collected, one about 5 km south of the entrance, and another about 1 km south of the entrance. The latter sample was collected during rising tide, and therefore represented water entering the Bay. The ^{228}Ra concentrations of the two samples were 0.8 and 2.0 mBq/L respectively. ^{228}Ra in open ocean water is usually <0.5 mBq/L (Broecker *et al*., 1973), and it is possible that the higher ^{228}Ra activity in the water entering PPB represents a proportion of PPB water previously transported out of the Bay on the ebbing tide, returning on the flood tide. Pattiaratchi *et al*. (1996) calculated that 3-5% of PPB water leaving the Bay returns on the following tide. Based on this calculation we have assigned a nominal ^{228}Ra concentration of 0.5 mBq/L to Bass Strait water. Since $c_{wc} >> c_{BS}$, the error in t_w resulting from the uncertainty in the ^{228}Ra content of Bass Strait water is small.

Other values assigned to parameters in equation (17) are 17.1 ±1.4 mBq/L for c_{wc} (the mean of measurements from the five sites), 13.5 m for H (the average PPB depth), and 34 ±3 mBq/cm^2/y as the Bay-wide average $^{228}F_s$ (the mean of fluxes from the three cores from Central and Northern PPB). Using these values, t_w is calculated to be 0.72 ±0.08 y (262 ±29 d). Implicit in this estimate of t_w is the assumption that $^{228}F_s$ is spatially constant in the Bay. As discussed in the previous section, it is possible that the region of the Bay where sand and gravel sediments dominate (about 25% of the area of the Bay) may have a lower value of $^{228}F_s$. Constraints on t_w can obtained by assuming the flux from this region lies between the Central Bay flux (34 mBq/cm^2/y) and zero. The assumption of zero flux from sand and gravel sediments yields an upper estimate of 0.96 ±0.11 y, and t_w is constrained to lie in the range 0.64 to 1.07 y (234-390 d). Clearly, this range could be reduced considerably by the analysis of more sediment samples from different regions of the Bay.

5. CONCLUSIONS

Sediment cores in Central PPB show evidence of post-depositional mixing, thereby limiting the effectiveness of sedimentation rate determinations using ^{210}Pb and ^{228}Th. The sedimentation rate is found to be <0.9 mm/y (0.034 g/cm^2/y) in the top 10 cm (and probably 20 cm) of Central Bay sediments. The mean mixing coefficient in this depth interval is 490 ±50 mm^2/y. Below 20 cm, sediment mixing may be more rapid, and mixing may be occurring as deep as 60 cm.

The mean residence time of particles in the Central Bay water column at the time of this study, estimated from the rate of removal of ^{228}Th, is 10 ±2 days. Based on this time, the normalised flux of suspended sediment to the floor of Central PPB is 0.145 ±0.022 g/cm^2/y. This estimate exceeds the maximum sedimentation rate derived using ^{210}Pb and ^{228}Th in cores by a factor of more than four, indicating that >80% of suspended particles in PPB are resuspended bottom sediments.

The PPB water column was vertically well-mixed on the time scale of about 1.5 days in areas other than Central Bay. In Central Bay there is evidence of inhibited mixing of bottom water on one sampling occasion, indicating the presence of a pycnocline.

The flux of ^{224}Ra from bottom sediments is 4 times greater than the flux attributable to molecular diffusion, indicating significant exchange of surface water and porewater by advective processes such as bioirrigation. Based on the ^{224}Ra content of porewater, the flux of porewater across the sediment-water interface in Central Bay is 6.8 x 10^{-5} cm^3/cm^2/s.

From ^{228}Ra mass balance, the residence time of water in the Bay lies in the range 0.64-1.07 years. The analysis of more sediment samples is required to further constrain this estimate.

6. ACKNOWLEDGMENTS

We thank John Barry (VFRI), Gary Caitcheon (CSIRO), and divers Mark Ferrier and Brett Abbot (VFRI) for their invaluable assistance with sample collection. Andy Longmore (VFRI) arranged additional sampling and provided additional suspended sediment data. David Smith (University of Melbourne) loaned sampling equipment and provided helpful advice on sampling strategy. Boda Obradovic and Matthew Rake (CSIRO) assisted with laboratory analysis of samples.

Melbourne Water, through the Port Phillip Bay Environmental Study funded this study.

7. REFERENCES

Appelby, P.G. and Oldfield F. (1983). The assessment of 210Pb data from sites with variable accumulation rates. *Hydrobiologia*, **103**, pp 29-35.

Appelby, P.G. and Oldfield F. (1992). Application of lead-210 to sedimentation studies. In: *Uranium-series Disequilibrium: Applications to Earth, Marine and Environmental Sciences*, M. Ivanovich and R.S. Harmon eds., pp 731-778, Clarendon press, 1992.

Beasley, A.W. (1966). Port Phillip Bay survey, 1957-1963: bottom sediments. *Memoirs of the National Museum of Victoria*, **27**, pp 69-105.

Berelson, W.M., Kilgore, T.E. and Heggie, D.T. (1994). Benthic chambers, nutrient fluxes and the biogeochemistry of the seafloor from Port Phillip Bay, Australia. AGSO Record 1994/16, Australian Geological Sciences Organisation.

Bird, L.F., Ford, P. and Heislers, S. (1996). Bioturbation by common Port Phillip Bay benthic invertebrates. Technical Report No. 37, CSIRO Port Phillip Bay Environmental Study, Melbourne.

Broecker W.S., Kaufman, A. and Trier R.M. (1973). The residence time of thorium in surface sea water and its implications regarding the rate of reactive pollutants. *Earth and Planetary Science Letters*, **20**, pp 35-44.

Bollinger M.S. and Moore W.S. (1993). Evaluation of salt marsh hydrology using radium as a tracer. *Geochimica and Cosmochimica Acta*, **57**, pp 2203-2212.

Chistensen, E.R. (1982). A model for radionuclides in sediments influenced by mixing and compaction. *Journal of Geophysical Research*, **87**, pp 566-572.

Greilach, P., You, K., Black, K. and Gorman, R. (1996). Sediment characteristics in Port Phillip Bay. Technical Report No. 23, CSIRO Port Phillip Bay Environmental Study, Melbourne.

Hancock G.J. and Murray A.S. (1996). The source and distribution of dissolved radium in the Bega River estuary, southeastern Australia. *Earth and Planetary Science Letters*, **138**, pp 145-155.

Harris, G., Batley, G., Fox, D., Hall, D., Jernakoff, P., Molloy, R. Murray A.,Newell, B., Parslow, G., Skyring, G., and Walker, S. (1996). Port Phillip Bay Environmental Study final report, CSIRO Canberra.

Huh, C-A., Zahnle, D.L., Small, L.F. and Noshkin, V.E. (1987). Budgets and behaviours of uranium and thorium series isotopes in Santa Monica Basin sediments. *Geochimica and Cosmochimica Acta*, **51**, pp 1743-1754.

Hunter, J.R. (1994), CSIRO Division of Oceanography. Personal communication, "Modelling of ^{210}Pb and TBT profiles in cores", Hobart, September 8, 1994.

Invanovich M. and Harmon, R.S. (1992). *Uranium-series Disequilibrium: Applications to Earth, Marine and Environmental Sciences*, 910 pages, Clarendon press, 1992.

Kasemsupaya, V., Tsobota, H. and Nozaki, Y. (1993). ^{228}Ra and its implications in the Seto Inland sea. *Estuarine and Coastal Shelf Science*, **36**, pp 31-45.

Koide, M., Bruland, K.W. and Goldberg E.D. (1973). Th-228/Th-232 and Pb-210 geochronolgies in marine and lake sediments. *Geochimica and Cosmochimica Acta*, **37**, pp 1171-1187.

Krishnaswami, S., Benninger, L.K., Aller, R.C. and Von Damm, K.L. (1980). Atmospherically-derived radionuclides as tracers of sediment mixing and accumulation in near-shore marine and lake sediments: evidence from ^{7}Be, ^{210}Pb and ^{239,240}Pu. *Earth and Planetary Science Letters*, **47**, pp 308-318.

Lerman, A. and Lietze, T.A. (1975). Uptake and migration of tracers in lake sediments. *Limnology and Oceanography*, **20**, pp 497-510.

Li Y-H., Feely, H.W. and Sanstchi, P.H. (1979). ^{228}Th-^{228}Ra disequilibrium in the New York Bight and its implications for coastal pollution. *Earth and Planetary Science Letters*, **42**, pp 13-26.

Longmore, A.R., Cowdell, R.A. and Flint, R. (1996). Nutrient status of water in Port Phillip Bay. Technical Report No. 24, CSIRO Port Phillip Bay Environmental Study, Melbourne.

Martin P. and Hancock, G.J. (1992) Routine analysis of naturally occurring radionuclides in environmental samples by alpha-particle spectrometry, Research Report 7, Supervising Scientist for the Alligator Rivers Region, AGPS, Canberra, Australia.

Martin P. and Akber, R.A. (1996). Groundwater seepage from the Ranger uranium mine tailings dam: Radioisotopes of radium thorium and actinium. Supervising Scientist Report 106, Supervising Scientist for the Alligator Rivers Region, AGPS, Canberra, Australia.

Moore, W.S. (1992). Radionuclides of the uranium and thorium decay series in the estuarine environment. In: *Uranium-series Disequilibrium: Applications to Earth, Marine and Environmental Sciences*, M. Ivanovich and R.S. Harmon eds., pp 396-422, Clarendon press, 1992.

Nicholson, G.J., Longmore A.R. and Cowdell R.A. (1996). Nutrient status of the sediments in Port Phillip Bay. Technical Report No. 26, CSIRO Port Phillip Bay Environmental Study, Melbourne.

Nozaki, Y., Horibe Y. and Tsubota, H. (1981). The water column distributions of thorium isotopes in the western North Pacific. *Earth and Planetary Science Letters*, **54**, pp 203-216.

Olley, J.M., Murray, A.S., Mackenzie, D.H. and Edwards, K. (1993). Identifying sediment sources in a gullied catchment using natural and anthropogenic radionuclides. *Water Resources Research*, **29**, pp 1037-1043.

Osmond J.K. and Cowart J.B. (1992). Ground water. In: *Uranium-series Disequilibrium: Applications to Earth, Marine and Environmental Sciences*, M. Ivanovich and R.S. Harmon eds., pp 731-778, Clarendon press, 1992.

Otto, C.J., (1992). Literature and information review of groundwater input of nutrients and toxicants to Port Phillip Bay. Technical Report No. 4, CSIRO Port Phillip Bay Environmental Study, Melbourne.

Pattiaratchi, C., Phillips, R., Oldham C. and Perkins A. (1996). Mixing, flushing and CTD surveys of the waters of Port Phillip Bay. Technical Report No. 34, CSIRO Port Phillip Bay Environmental Study, Melbourne.

Robbins, J.A. (1978). Geochemical and geophysical applications of radioactive lead. In: *The Biogeochemistry of Lead in the Environment*, Part A, ed. J.O. Nriagu. pp 285-393, Elsevier Scientific, Amsterdam.

Robbins, J.A. and Edgington, D.N. (1975). Determination of recent sedimentation rates in Lake Michigan using Pb-210 and Cs-137. *Geochimica and Cosmochimica Acta*, **39**, pp 285-304.

Santschi, P.H., Li, Y-H. and Bell, J. (1979). Natural Radionuclides in the water of Narrangansett Bay. *Earth and Planetary Science Letters*, **45**, pp 201-213.

Thomson, J., Turekian, K.K. and McCaffrey, R.J. (1975). The accumulation and metals in and release from sediments of Long Island Sound. In: L.E. Cronin (ed.), Estuarine Research, Vol. 1, Academic Press, New York, pp 28-43.

Turekian, K.K., Tanaka, N., Turekian, V.C., Torgensen, T. and Deangelo, E.C. (1996). Transfer rates of dissolved tracers through estuaries based on ^{228}Ra: A study of Long Island Sound. *Continental Shelf Research*, **16**, No.7, pp 863-873.

Walker, S. J. and Sherwood, C.R. (1997). A Transport Model of Port Phillip Bay. Technical Report No. 39, CSIRO Port Phillip Bay Environmental Study, Melbourne.

Webster I.T., Hancock G.J. and Murray A.S. (1994). On the use of radium isotopes to examine pore water exchange in an estuary, *Limnology and Oceanography*, **39**, (8): pp 1917-1927.

Webster, I.T., Hancock, G.J. and Murray, A.S. (1995). Modelling the effect of salinity on the desorption of radium from sediments. *Geochimica and Cosmochimica Acta*, **59**, pp 2469-2476.

Wilson, R.S., Cohen, B.F. and Poore, G.C.B. (1993). The role suspension-feeding and deposit-feeding benthic macroinvertebrates in nutrient cycling in Port Phillip Bay. Technical Report No. 10, CSIRO Port Phillip Bay Environmental Study, Melbourne.

You Z., Greilach, P.R., Turnbull, J.F., Hatton, D.N. and Black, K.P. (1996). Field measurements of suspended sediment concentrations in Port Phillip Bay. Technical Report No. 28, CSIRO Port Phillip Bay Environmental Study, Melbourne.